# AMNIOTIC MEMBRANE BASED STRATEGIES FOR CORNEAL REGENERATION

by

**Fatma Zehra Erkoç Biradlı**

B.S., in Bioengineering, Yıldız Technical University, 2013

M.S., in Biomedical Engineering, Boğaziçi University, 2017

Submitted to the Institute of Biomedical Engineering

in partial fulfillment of the requirements

for the degree of

Doctor

of

Philosophy

Boğaziçi University

2024

# AMNIOTIC MEMBRANE BASED STRATEGIES FOR CORNEAL REGENERATION

## APPROVED BY:

Prof. Dr. Bora Garipcan .....
(Thesis Advisor)

Prof. Dr. Rıfat Rasier .....
(Thesis Co-advisor)

Prof. Dr. Esin Öztürk Işık .....

Assoc. Prof. Dr. Duygu Ege .....

Prof. Dr. Lokman Uzun .....

Assoc. Prof. Dr. Sedat Odabaş .....

**DATE OF APPROVAL:** 27 August 2024

# ACKNOWLEDGMENTS

My profound appreciation extends to my advisor Prof. Dr. Bora Garipcan, who supported me at every stage, provided guidance, moral support, and motivation throughout my Ph.D. study. His knowledge, patience, and encouragement were assisting in the accomplishment of this dissertation.

I am also grateful to my thesis co-advisor Prof. Dr. Rıfat Rasier for his support, guidance, invaluable insights. His clinical point of view has enabled my studies more application oriented and enriched the quality of the research.

I would like to express my gratitude to the members of my thesis committee, Prof. Dr. Esin Öztürk Işık, Assoc. Dr. Duygu Ege, Prof. Dr. Lokman Uzun, and Assoc. Prof. Dr. Sedat Odabaş for their helpful insights and feedback.

I would like express my thanks to the Council of Higher Education (YÖK) for Council of Higher Educational 100/2000 Ph.D Scholarship. The investigations conducted in this thesis were partially supported by fund from Bogazici University Research Fund (grant number 6701).

I thank all my friends and teammates in the institute, especially Berkay Erenay, Alp Özgün, Özgen Öztürk Öncel, Bengü Aktaş, Hatice Kaya and Şeyma Soykan for their support, motivation, and collaboration. I will always remember their support and intimate friendships that made my journey easier.

My heartfelt thanks to my husband, Celal, for his unwavering cooperation and his efforts to smooth my way all the time.

Finally, I am deeply grateful to my family for their unwavering belief in me and their boundless love. This thesis is dedicated to my father, whose steadfast faith in my

path to becoming a successful scientist has been a constant source of inspiration.

# ACADEMIC ETHICS AND INTEGRITY STATEMENT

I, Fatma Zehra Erkoç Biradlı, hereby certify that I am aware of the Academic Ethics and Integrity Policy issued by the Council of Higher Education (YÖK) and I fully acknowledge all the consequences due to its violation by plagiarism or any other way.

Name :

Signature:

Date:

# ABSTRACT

## AMNIOTIC MEMBRANE BASED STRATEGIES FOR CORNEAL REGENERATION

Human amniotic membrane (HAM), obtained from the inmost layer of the placenta, has been utilized in tissue engineering and regenerative medicine applications for many years in various forms such as intact HAM, decellularized, micronized or extract form. Amniotic membrane extract (AME) is an extract form of HAM and known to contain a plethora of cytokines and growth factors, making it a highly attractive option for topical applications. In the first part of thesis, the effects of AME concentration on corneal keratocytes and the effects of using AME with eye drops on cell viability were investigated. It has been observed that the combined use of 50 $\mu g$/mL AME and eye drops increases corneal keratocyte cell proliferation. In the second part of thesis, AME was blended with Wharton's jelly mesenchymal stem cells derived-exosomes (WJ-MSC-Exos) and the effects of their combined use on the proliferation of corneal keratocytes as well as their ability to promote *in vitro* cell migration, wound healing, and their impact on cellular morphology were evaluated. Although WJ-MSC-Exos and AME have been used separately for wound healing research, their combined synergistic effects have not been studied extensively. Our findings indicated that the presence of both exosomes (3x$10^5$ Exo/mL) and AME (50 $\mu g$/mL) synergistically enhance the proliferation of corneal keratocytes. Overall, all these findings demonstrate that HAM can be utilized towards corneal regeneration through various strategies, or in combination with helpful solutions such as exosomes and eye drops.

**Keywords:** Wharton's Jelly Mesenchymal Stem Cells Derived Exosomes, Amniotic Membrane Extract, Corneal Keratocytes, Eye Drops, *In vitro* Corneal Wound Healing.

# ÖZET

## KORNEA REJENERASYONUNA YÖNELİK AMNİYOTİK MEMBRAN TEMELLİ STRATEJİLER

Plasentanın en içtabakasından elde edilen insan amniyotik membranı (İAM), hücresizleştirilmiş, mikronize edilmiş veya ekstrakt formunda olmak üzere çeşitli formlarda doku mühendisliği ve rejeneratif tıp uygulamalarında uzun yıllardan beri kullanılmaktadır. Amniyotik membran ekstraktı (AME), İAM'nın bir ekstrakt formudur ve bol miktarda sitokin ve büyüme faktörü içerdiği bilinmektedir, bu da AME'nı topikal uygulamalar için oldukça cazip bir seçenek haline getirmektedir. Tezin ilk bölümünde, AME'nın farklı konsantrasyonlarda kornea keratositleri üzerindeki etkileri ve AME'nın yapay göz damlası ile birlikte kullanılmasının hücre canlılığı üzerine etkileri araştırılmıştır. 50 $\mu g$/mL AME ile göz damlasının birlikte kullanımının kornea keratosit hücre çoğalmasını arttırdığı gözlemlenmiştir. Tezin ikinci bölümünde AME, Wharton Jölesi mezenkimal kök hücrelerinden elde edilen eksozomlar (WJ-MKH-Eksozomlar) ile kombine edilmiş ve kombine kullanımının kornea keratositlerinin çoğalması üzerindeki etkilerinin yanı sıra *in vitro* hücre migrasyonunu ve yara iyileşmesini destekleme yetenekleri ve hücresel morfoloji üzerindeki etkileri araştırılmıştır. Her ne kadar WJ-MKH-Eksozomlar ve AME yara iyileştirme araştırmalarında ayrı ayrı kullanılmış olsa da, kombine sinerjistik etkileri kapsamlı bir şekilde araştırılmamıştır. Bulgularımız, hem eksozomların (3x$10^5$ Exo/mL) hem de AME'nın (50 $\mu g$/mL) varlığının, kornea keratositlerinin proliferasyonunu sinerjistik olarak arttırdığını göstermektedir. Genel olarak, tüm bu bulgular İAM'nın çeşitli stratejiler yoluyla veya eksozomlar ve göz damlaları gibi yardımcı çözeltilerle kombinasyon halinde kornea rejenerasyonuna yönelik olarak kullanılabileceğini göstermektedir.

**Anahtar Sözcükler:** Wharton Jölesi Mezenkimal Kök Hücrelerinden Elde Edilen Eksozomlar, Amniyotik Membran Ekstraktı, Kornea Keratositleri, Göz Damlası, *İn vitro* Kornea Yara İyileşmesi.

# TABLE OF CONTENTS

ACKNOWLEDGMENTS . . . . . iii
ACADEMIC ETHICS AND INTEGRITY STATEMENT . . . . . v
ABSTRACT . . . . . vi
ÖZET . . . . . vii
LIST OF FIGURES . . . . . xi
LIST OF SYMBOLS . . . . . xiv
LIST OF ABBREVIATIONS . . . . . xv
1. INTRODUCTION . . . . . 1
1.1 Motivation . . . . . 3
1.2 Objectives and Outline of the Thesis . . . . . 3
2. BACKGROUND . . . . . 5
2.1 The Structure and Functions of Cornea . . . . . 5
2.2 Cell Types in Cornea . . . . . 7
2.2.1 Corneal Keratocytes . . . . . 8
2.3 Corneal Wound Healing . . . . . 9
2.4 Human Amniotic Membrane (HAM) . . . . . 9
2.4.1 HAM in Tissue Engineering and Regenerative Medicine Applications . . . . . 11
2.5 Artificial Tears . . . . . 13
2.6 Exosomes . . . . . 13
3. THE EFFECTS OF COMBINED USE OF AMNIOTIC MEMBRANE EXTRACT AND EYE DROP ON CORNEAL KERATOCYTE CELLS (PRELIMINARY STUDIES) . . . . . 17
3.1 Storage of Fresh Human Amniotic Membrane (HAM) . . . . . 17
3.2 Characterization and Processing of Fresh Human Amniotic Membrane . 18
3.2.1 Scanning Electron Microscopy (SEM) Analysis . . . . . 18
3.2.2 Hematoxylin and eosin (HE) staining . . . . . 19
3.3 Preparation and Characterization of Gelatin-HAM Biocomposite Hydrogels . . . . . 20

3.4 Preparation of AME . . . . . 21
3.5 Characterization of AME . . . . . 22
3.6 Cytocompatibility of AME and Combined Use of AME and Eye Drop . 23
3.7 Findings of the Preliminary Experiments . . . . . 24
3.7.1 Characterization Results of Human Amniotic Membrane . . . . 24
3.7.2 SEM Characterization Results of Gelatin-HAM Biocomposites . 24
3.7.3 Characterization of AME . . . . . 27
3.7.4 Cytocompatibility of AME and Combined Use of AME and Eye Drop . . . . . 28
3.8 Discussion . . . . . 30
4. MESENCHYMAL STEM CELLS DERIVED-EXOSOMES ENHANCED AMNIOTIC MEMBRANE EXTRACT PROMOTES CORNEAL KERATOCYTE PROLIFERATION . . . . . 33
4.1 Preparation and Characterization of AME . . . . . 33
4.2 Characterization of WJ-MSC-Exos . . . . . 34
4.2.1 Dynamic Light Scattering (DLS) Measurements for Exo . . . . 35
4.2.2 Scanning Electron Microscopy Analysis of Exo . . . . . 35
4.3 Cytocompatibility of AME and Exo . . . . . 35
4.3.1 MTT assay . . . . . 35
4.3.2 alamarBlue Cell Proliferation Assay . . . . . 36
4.4 Actin Cytoskeleton and Nuclei Staining . . . . . 36
4.5 *In Vitro* Scratch Assay/ Cell Migration Assay . . . . . 37
4.6 Statistical Analysis . . . . . 37
4.7 Results . . . . . 38
4.7.1 Characterization of AME . . . . . 38
4.7.2 Characterization of Exo . . . . . 38
4.7.3 Cytocompatibility of AME and Exo . . . . . 38
4.7.3.1 MTT Assay . . . . . 38
4.7.3.2 alamarBlue Assay . . . . . 39
4.7.4 Actin Cytoskeleton and Nuclei Staining (Phalloidin/DAPI Staining) . . . . . 41
4.7.5 *In Vitro* Scratch Assay / Cell Migration Assay . . . . . 43

4.8 Discussion . . . . . 46
5. CONCLUSION . . . . . 51
APPENDIX A. CALIBRATION CURVES . . . . . 52
REFERENCES . . . . . 53

# LIST OF FIGURES


| | | |
|---|---|---|
| Figure 2.1 | The Structure and Layers of the Cornea [33]. | 6 |
| Figure 2.2 | Outline depiction of the structure of Human Amniotic Membrane (HAM) [1]. | 10 |
| Figure 2.3 | Illustrative depiction of the process of exosome formation and the molecular cargo involved [73]. | 14 |
| Figure 2.4 | The classification of exosomes based on their source (adapted from)[18]. | 15 |
| Figure 3.1 | Storage of Fresh Human Amniotic Membrane (HAM). | 18 |
| Figure 3.2 | Fresh HAM before characterization studies. | 19 |
| Figure 3.3 | Preparation of Amniotic Membrane Extract (AME) solution. | 22 |
| Figure 3.4 | Cross-sectional SEM images of lyophilized HAM. Scale bar: 50 $\mu m$(A), 5 $\mu m$ (B). | 26 |
| Figure 3.5 | SEM images of fresh Human Amniotic Membrane. Scale Bar: 30 $\mu m$ and 3 $\mu m$ respectively. | 27 |
| Figure 3.6 | Haematoxylin-Eosin Staining of Human Amniotic Membrane. Scale bar 10 $\mu m$ (A), 10 $\mu m$(B). | 27 |
| Figure 3.7 | Cross-sectional SEM images of gelatin sponge and pore sizes. | 28 |
| Figure 3.8 | Cross-sectional SEM images of Gelatin-HAM Biocomposite (3:1 Gelatin:HAM ratio) Scale bar 500 $\mu m$(A), 200 $\mu m$(B). | 29 |
| Figure 3.9 | Cross-sectional SEM images of Gelatin-HAM Biocomposite (5:1 Gelatin:HAM ratio). Scale bar 500 $\mu m$(A), 200 $\mu m$(B). | 29 |
| Figure 3.10 | MTT Assay Results 1 and 2 days after AME and Eye Drop Application. | 30 |
| Figure 4.1 | Graphical abstract of experimental procedures. In this part of the study AME have been combined with WJ-MSC-Exos. Corneal keratocyte behavior was observed to be enhanced after optimization of mixture concentrations. Created with BioRender.com | 34 |

Figure 4.2 Characterization of WJ-MSC-Exos. A) DLS measurement for Exo size distribution by number %, B) DLS measurement for Exo size distribution by intensity %, C) SEM image of WJ-MSC-Exos (Scale bar: 500 nm). 39

Figure 4.3 Results of MTT assay on L929 fibroblast cells treated with 700 $\mu g$/mL, 280 $\mu g$/mL, 140 $\mu g$/mL, 70 $\mu g$/mL, and 28 $\mu g$/mL, 14 $\mu g$/mL AME after 48 hours. (ns: $p \geq 0.05$). 40

Figure 4.4 Cell proliferation results for corneal keratocytes, assessed by alamarBlue assay. A) Cell proliferation of corneal keratocytes treated with $3x10^5$ Exo/mL and $3x10^6$ Exo/mL (days 1, 2, and 3). B) Cell proliferation of corneal keratocytes treated with $3x10^5$, 50 $\mu g$/mL AME and 50 $\mu g$/mL AME + $3x10^5$ Exo/mL (days 1, 2, and 3). (ns: $p \geq 0.05$, ****: $p < 0.0001$). Cell proliferations are normalized to day 1 vehicle control. 41

Figure 4.5 Fluorescent staining of adherent human corneal keratocytes at day 2 on tissue culture plates treated with 50 $\mu g$/mL AME, $3x10^5$ Exo/mL, 50 $\mu g$/mL AME and $3x10^5$ Exo/mL, vehicle control (serum free culturing medium), and vehicle+ FBS (culturing medium contains 10% FBS), stained with conjugated phalloidin (Alexa Fluor™ 488 Phalloidin) and DAPI, Green colour indicates the actin cytoskeleton and blue colour indicates the nuclei. Scale bars: 50 $\mu m$. 42

Figure 4.6 Scratch assay on corneal keratocytes depicting wound closure ratios after treatments with 50 $\mu g$/mL AME, $3x10^5$ Exo/mL and 50 $\mu g$/mL AME+ $3x10^5$ Exo/mL. A) Representative cell images at initial wound creation and after 24 hours of treatment. (Scale bar: 500 $\mu m$) B) Wound Closure ratio (%). Scratch assay on corneal keratocytes indicates significantly higher wound closure in cells treated with 50 $\mu g$/mL AME + $3x10^5$ Exo/mL compared to cells treated with only $3x10^5$ after 24 hours (*$p < 0.05$). 44

Figure 4.7 Fluorescent staining of adherent human corneal keratocytes on tissue culture plates after scratch assay showing that cell migration after treatments with 50 $\mu g$/mL AME, 3x$10^5$ Exo/mL and their mixture. Images were taken 48 hours after the creation of the wound. Green colour indicates the actin cytoskeleton and blue colour indicates the nuclei (Scale bar: 200 $\mu m$). 45

Figure A.1 Calibration curve for Pierce™ BCA Protein Assay generated to determine AME concentration (Second batch of AME aliquots). 52

# LIST OF SYMBOLS

| | |
|---|---|
| °C | Degree Celcius |
| HCl | Hydrochloric Acid |
| NaOH | Sodium Hydroxide |
| $\mu g$ | Microgram |
| $\mu L$ | Microliter |
| mg | Milligram |
| mL | Milliliter |
| mM | Millimolar |
| $\mu m$ | Micrometer |
| rpm | Round per minute |

# LIST OF ABBREVIATIONS

| | |
|---|---|
| AM | Amniotic Membrane |
| AME | Amniotic Membrane Extract |
| ANOVA | Analysis of Variance |
| BSA | Bovine Serum Albumin |
| BMP5 | Bone Morphogenetic Protein 5 |
| BMP7 | Bone Morphogenetic Protein 7 |
| CEnCs | Corneal Endothelial Cells |
| DAPI | 4,6-diamidino-2-phenylindole |
| DLS | Dynamic Light Scattering |
| DMEM | Dulbecco's Modified Eagle Medium |
| DMSO | Dimethyl Sulfoxide |
| ECM | Extracellular Matrix |
| EGF | Epithelial Growth Factor |
| EGF-R | Epidermal Growth Factor Receptor |
| Exo | Exosome |
| FBS | Fetal Bovine Serum |
| FGF4 | Fibroblast Growth Factor 4 |
| GelMA | Methacrylated Gelatin |
| HAM | Human Amniotic Membrane |
| HCECs | Human Corneal Epithelial Cells |
| HE | Hematoxylin and Eosin |
| HGF | Hepatocyte Growth Factor |
| HA | Hyaluronic acid |
| IL-1RA | Interleukin-1 Receptor Antagonist |
| KGF | Keratinocyte Growth Factor |
| MSC | Mesenchymal Stem Cell |
| PBS | Phosphate Buffered Saline |
| PDI | Polydispersity Index |

| | |
|---|---|
| PlGF | Placental Growth Factor-1 |
| PVA | Polyvinyl Alcohol |
| WJ-MSC-Exo | Wharton's Jelly Mesenchymal Stem Cells Derived Exosomes |
| SEM | Scanning Electron Microscopy |
| TCP | Tissue Culture Plate |
| TGF-$\beta$ | Transforming Growth Factor-Beta |
| VEGF | Vascular Endothelial Growth Factor |

# 1. INTRODUCTION

Human amniotic membrane (hAM) has been one of the most frequently utilized natural materials in tissue engineering and regenerative medicine applications in various forms for more than hundred years. It has been used for wound treatment, repair of tissues, such as tendon, skin, cornea, nerve, cartilage, and oral mucosa. hAM has an avascular and a five-layered structure. hAM is naturally available, relatively inexpensive, and a biocompatible material [1–3]. Recently, contrary to its conventional direct use as fresh, unprocessed membrane after its inception, various processing methods have been applied to hAMs; such as drying, laminating [4], decellularization, micronization [5], and deriving an extract [6]. In addition, numerous composites that contain polymeric materials and different forms of hAM have been produced [7]. For instance, double layered membrane which contains chitosan sponge and decellularized hAM have been used to boost diabetic wound healing [8]. In another study, decellularized hAM attached polyvinyl alcohol (PVA) hydrogels were investigated as an artificial corneal scaffold [9]. Methacrylated gelatin (GelMA) hydrogels that contained decellularized hAM particles have been synthesized as composite material for oral mucosa repair [10].

Due to its varying thickness and transparency, fresh hAM is considered as a non-homogeneous material. Additionally, surgical manipulation and suturing of hAM can become technically challenging, which spurred the formation of AME as a more streamlined hAM product [11]. AME contains a plethora of cytokines and growth factors, such as, epithelial growth factor (EGF), keratinocyte growth factor (KGF), hepatocyte growth factor (HGF), and interleukin-1 receptor antagonist (IL-1RA), bone morphogenetic protein 5 (BMP5), bone morphogenetic protein 7 (BMP7), epidermal growth factor receptor (EGF-R), fibroblast growth factor 4 (FGF4), insulin-like growth factor binding protein (IGFBP1-6), placental growth factor-1 (PlGF), transforming growth factor beta 1 (TGF$\beta$1), vascular endothelial growth factor (VEGF) [12, 13]. Many of these aforementioned growth factors which are existed in AME, such as,

EGF, TGF$\beta$1, HGF, insulin-like growth factor (IGF) and KGF participate actively in corneal wound healing process [14]. In the investigation carried out by Guo *et al.*, when amniotic membrane homogenate and amniotic membrane have been compared in terms of their effectiveness on corneal repair in the rabbit model, the statistical comparison between the homogenate and membrane group revealed no significant difference. This result proves that the effectiveness of amniotic membrane homogenate [15].

Exosomes can be defined as a type of extracellular vesicle having a diameter of around 30-200 nm [16]. Although their physiological roles are not entirely understood, it is thought that they contribute to intercellular signalling to maintain cellular homeostasis and to remove waste products from the cells. They are similar to complex cargo molecules and have some components such as DNA, RNA, metabolites, and cell membrane proteins. These characteristics enable exosomes to be employed for both diagnostic evaluations and therapeutic interventions in clinical settings [17]. Exosomes can be made by almost all type of cells, in both healthy environments and tumour conditions [18]. Exosomes are also known to help regulate the wound healing process through specific signalling pathways [19]. Exosomes derived from varieties of cells, such as corneal mesenchymal stromal cells, corneal epithelial cells and induced pluripotent stem cells (iPSCs), were investigated for their effects on corneal wound healing [20–22]. MSCs-Exos and iPSCs-Exos can restrain apoptosis of human corneal epithelial cells (HCECs), stimulate cellular proliferation and migration of HCECs *in vitro*. They also facilitate wound repair *in vivo* [22]. These promising effects of exosomes in wound healing, obtained from the aforementioned cell sources, may extend towards another source, namely WJ-MSC-Exos. These types of exosomes are obtained from MSCs found in WJ which is a connective tissue found in umbilical cords. These types of mesenchymal stem cells are younger compared to cells found in adipose and bone marrow tissues, making them relatively more protected to aging related damages [23]. Recently, WJ-MSC-Exos are reported to promote cutaneous wound healing [24].

## 1.1 Motivation

Exosomes and amniotic membrane have been used together in the past for wound healing research. Adipose derived mesenchymal stem cells exosome-incorporated with hAM were investigated in terms of their efficiency for the recovery of diabetic skin injuries *in vivo*, which resulted in expedited wound healing in diabetic mice [25]. Recently, umbilical cord-derived MSCs, which are a prospective source of exosomes, have been used alongside of micronized amniotic membranes and resulted in a significantly accelerated burn wound healing response [26]. To date, no investigation has been conducted to assess the combined utilization of the hAM in an extract form (AME) and WJ-MSC-Exos, both of which individually exhibit substantial effects on the wound healing process. Furthermore, both of these sources are from fetal environments, which may further enhance their currently established effects on wound healing due to rich growth factor and protein presence.

In this thesis, the isolated and synergistic effects of AME and WJ-MSC-Exos on corneal keratocytes were investigated in terms of cell proliferation, cellular morphology, cell migration behavior and *in vitro* wound healing efficiency. Beforehand, the combined use of AME and artificial eye drops on corneal keratocytes were also evaluated in terms of cell proliferation. Artificial eye drops are also known to have beneficial effects on corneal wound recovery.

## 1.2 Objectives and Outline of the Thesis

The primary focus of this thesis is to facilitate corneal regeneration utilizing human amniotic membrane with different strategies. The thesis includes two main study parts. In the first part of the study that was given in Chapter 3, HAM was obtained, stored in appropriate conditions, characterization studies were performed to learn the material. Then HAM was micronized and incorporated into gelatin hydrogels to obtain gelatin-HAM biocomposites. Characterization of obtained biocomposite materials

was performed using Scanning Electron Microscopy (SEM). This part of the study can be attributed as preliminary studies. In the later stage of the study, it is decided to use amniotic membrane extract (AME) for the remaining studies to obtain more homogeneous distribution of HAM content. AME prepared and characterized, then the effects of AME concentration (14-700 $\mu g$/mL) on expansion of cultured human corneal keratocytes were investigated. The effects of application of AME with preservative-free eye drops (ED) on cultured human corneal keratocytes were investigated.

In Chapter 4, exosomes originating from WJ-MSC were included in the study and the effects of AME and WJ-MSC-Exos, both individually and in combination, on the proliferation of corneal keratocytes were investigated. Additionally, their ability to promote *in vitro* cell migration and wound healing, as well as their impact on cellular morphology, were examined.

Objectives of the thesis are as follows:

- Inclusive summary of the literature about the usage of HAM in various forms for applications in regenerative medicine and tissue repair, particularly corneal regeneration.
- Characterization and micronization of HAM.
- Production of biocomposites containing micronized HAM and gelatin.
- Investigating the impacts of AME in different concentrations on corneal keratocytes and the effects of using AME with eye drops on corneal keratocyte cell viability.
- Evaluation of the isolated and synergistic impacts of AME and WJ-MSC-Exos on corneal keratocytes in terms of cell proliferation, cellular morphology, cell migration behaviour and *in vitro* wound healing efficiency.

# 2. BACKGROUND

## 2.1 The Structure and Functions of Cornea

The human eye is a sophisticated organ with primarily responsible for vision. Anatomically, the eye contains three main zones: the outer fibrous layer, the middle vascular layer, and the inner neural layer. Cornea and sclera form the outer layer of the eye. The choroid, ciliary body, and iris constitute the middle layer. The inner neural layer, the retina, is composed of complex and layered neurons that gather and transform the light [27].

The human cornea is non-vascular and transparent tissue that serves as protective barrier. The horizontal diameter of the cornea is about 11-12 mm, and its vertical measurement is 9-11 mm. The average corneal diameter of the cornea in males and females is similar [28]. Beyond its roles as a structural barrier for infectious agents, it also contributes refractive capability of the eye. The human cornea is composed five distinct layers, the epithelium, Bowman's layer, stroma, Descemet's membrane, and endothelium [29]. The structure and strata of the cornea were shown in Figure 2.1.

The corneal epithelium comprises 10% of total cornea and its total thickness is about 53 $\mu m$ [30]. The epithelium consists of five to seven layers of cells and serves as a barrier for both preventing the incoming pathogens and sustaining dehydrated state of the cornea. In addition, it has crucial function in refractive capability of the eye. Corneal epithelial cells' time of life is approximately 7-10 days, then they go through apoptosis, and they are recreated by limbal stem cells at limbus [29].

Epithelial Basement Membrane is placed above the Bowman's layer and contains Type IV collagen, laminin, anchoring fibrils, anchoring plaques and many extracellular matrix molecules. Epithelial Basement Membrane has important function in controlling epithelial cells' migration and differentiation behaviour via regulating local

concentrations of growth factors and cytokines [31, 32].

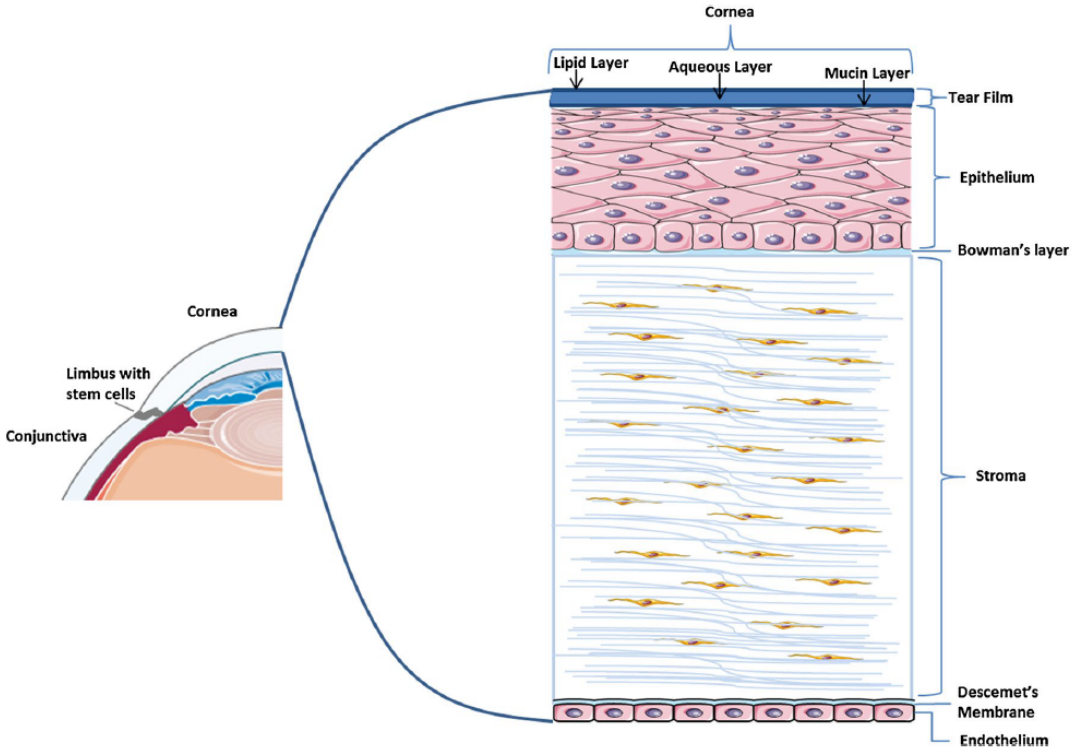


**Figure 2.1** The Structure and Layers of the Cornea [33].

Bowman's Layer is subepithelial collagenous layer, which is named after its discoverer, William Bowman. Bowman's layer has been found in human and some species, but not found in all species. No harmful effects have been observed in a large number of patients who have had the Bowman layer in the center of the cornea removed [34].

The stroma constitutes 90% of corneal volume, so it is the thickest layer of the cornea. Its thickness is nearly 500 $\mu m$ in human. The stroma consists of collagen fibers network, and extracellular matrix containing water, inorganic salts, proteoglycans, and glycoproteins. Important functions of the stroma include maintaining transparency, shape and structural integrity. Corneal keratocytes are the prevailing cell type in the corneal stroma [35].

Descemet's membrane (DM) is a subjacent layer of corneal endothelium. It helps

sustaining corneal transparency by controlling hydration and serves as the basement membrane for the corneal endothelium. DM involves many ECM components such as laminins, collagen type IV, nidogens and perlecan. These elements are present in the majority of basement membranes. In addition, it is known that the DM specifically contains collagen VIII and that this structure contributes to the formation of the hexagonal mesh structure [36]. Its thickness is about 8-10 $\mu m$ and elastic modulus of this soft membrane is between 0.23-2.6 kPa [37].

Corneal endothelium consists of polygonal, mostly hexagonal corneal endothelial cells (CEnCs) monolayer. These cells have fundamental function in maintaining corneal transparency via fluid transporting. Since CECs have limited proliferation capacity *in vivo*, cell density can decrease due to several reasons like some genetic disorders, aging, trauma after surgical operations, and glaucoma. When cell density falls below the critical level, corneal endothelium loses its function. Corneal edema occurs and eventually it can be resulted in vision loss [38, 39].

## 2.2 Cell Types in Cornea

The human cornea includes cellular elements such as epithelial cells, keratocytes, and endothelial cells and also contains components like collagen and glycosaminoglycans [29]. Corneal diseases, corneal damage and scar formation are crucial problems that can lead vision loss or blindness. Recovery strategies include mainly transplantation and tissue engineered strategies, but when it comes to clinical use, most of these options can fall short to make a full recovery. At this point, stem cells have gained much attention to treat corneal impairments. Stem cells that are in cornea have been isolated, characterized and their potential to treatment of damaged corneal tissue have been started to investigate. Adult stem cells, which remain in specific areas or niches within tissues throughout the body, possess the capacity to self-renovate and differentiate. The identified stem cells in the cornea are mainly corneal epithelial stem cells (limbal epithelial stem cells), corneal stromal stem cells and corneal endothelial stem/progenitor cells. Corneal epithelial stem cells which also named as limbal epithe-

lial stem cells (LESCs) since they are located in limbus [40].

### 2.2.1 Corneal Keratocytes

Corneal keratocytes are normally quiescent cells with dendritic morphology that placed in corneal stroma. These mesenchymal derived cells includes highly expressed proteins, crystallins, which promote to the corneal transparency [41, 42]. In the resting state, corneal keratocytes are responsible for collagen synthesis and degradation, proteoglycan synthesis, and intercellular communication [43]. In case of corneal injury, the course of keratocytes take can vary along three different paths, depending on the nature of the injury. Following an injury, keratocytes are prompted to either go through cell death or shift from their quiescent state to adopt regenerative phenotypes. These regenerative phenotypes can play a dual role, either fostering regeneration or triggering the formation of fibrotic scars. The formation of fibrotic scars is particularly detrimental to the otherwise transparent structure of the cornea [44]. In a previous study, corneal stromal cell-based treatment strategy was used by directly injection of corneal stromal cells to avoid corneal opacity and reproduce corneal transparency in a rat model [45]. However, proliferation of corneal stromal cells from donors *in vitro*, under standard cell culture conditions is quite challenging. When serum or growth factors-supplement are added into cell culturing media, corneal keratocytes differentiate into corneal fibroblasts and lose their keratocyte characteristic features such as keratan or lumican expression [46]. Therefore, culturing corneal keratocytes while preserving their characteristics and morphology is a substantial issue that needs to be studied. A research carried out by Espana *et al.* reveals that culturing human corneal keratocyte on human amniotic membrane provides to retain keratocytes characteristic morphology and keratocan expression even in the existence of high serum concentrations (10%) [47]. Another research indicated that when they are cultured on stromal side of HAM, myofibroblasts could shift to fibroblast phenotype [48]. Amniotic membrane was also utilized as a corneal stromal equivalent with the addition of keratocytes. Ultrathin amniotic membrane layers with keratocytes were stratified to construct a corneal stromal equivalent and keratocytes again keep their characteristics phenotype on this layered

structure [49]. All these studies revealed that HAM has positive effects to avoid corneal haze. In this PhD thesis, corneal keratocytes were utilized as an *in vitro* cell model.

## 2.3 Corneal Wound Healing

It is known that the process of corneal wound healing is intricate, involving multiple cell types, growth factors, cytokines, and components of the immune system. Injury can be traumatic, infectious, disease-related or surgical. The wound healing process differs based on the type and extent of damage. Corneal epithelial, stromal and endothelial wound healing are examined separately. The healing of these cells is similar in a many of molecular processes. However, several actions vary significantly between corneal cell types [50]. If examined specifically in terms of stromal wound healing, the healing process progresses as follows: Following stromal injury, keratocytes in the region appear to undergo sudden apoptosis. Necrosis of some keratocytes occurs. Neighbour keratocytes start to proliferate and migrate. Then adjoining resting keratocytes change their phenotype and become active fibroblasts. Through the help of some growth factors like FGF-2 and PDGF-AB, TGF-$\beta$, fibroblasts turn into myofibroblasts. This transformation is sparked by TGF-$\beta$ [50, 51]. A large amount of tentative ECM was secreted by myofibroblasts. Epithelial and stromal cells generate pro-inflammatory chemokines which cause arrival of inflammatory cells. After the clearance of apoptotic and necrotic debris, the next stage is stroma remodelling. In this stage, irregular ECM is resorbed and myofibroblast go through apoptosis or reverse their phenotype. The stroma is gradually being restored [52].

## 2.4 Human Amniotic Membrane (HAM)

The fetus is protected by the fetal membrane, which comprises two parts: the uterine wall-facing chorion, and the amnion, which faces the amniotic fluid. The avascular HAM comprised of three layers. Closest to the amniotic fluid is a monolayer of

cuboidal epithelial with apically situated microvilli, called the amniotic epithelium. On the basal side of this amniotic epithelium is a basement membrane containing type-IV, V and VII collagen, and other structural molecules, including actin, $\alpha$-actinin, laminin, and vimentin. Beyond the basement membrane can be found a layer with mesenchymal fibroblast-like cells and is abundant in proteoglycans and glycoprotein. If viewed histologically, this layer looks spongy and is thus known as the zona spongiosa [53]. This layer is also named as a stroma and can be divide into three sub-groups: compact layer, fibroblast layer and spongy layer [1, 54]. Outline depiction of the structure of the HAM is shown in Figure 2.2 [1].

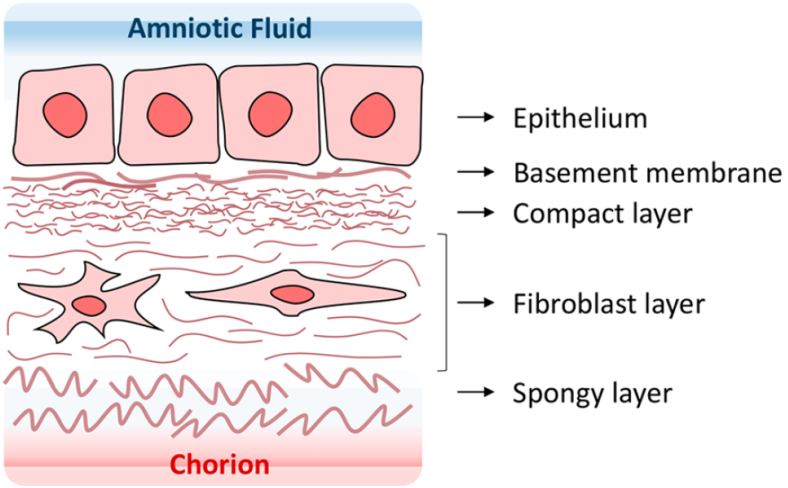


**Figure 2.2** Outline depiction of the structure of Human Amniotic Membrane (HAM) [1].

HAM is naturally available, relatively inexpensive, and biocompatible materials that is commonly utilized in in the field of tissue engineering and regenerative medicine more than a hundred years [2]. HAM has fibrosis-inhibiting, inflammation-reducing, angiogenesis-suppressing, and antibacterial properties. It is known that when HAM implanted into the body, it supports wound healing process and reduces scar. In addition, HAM promotes cell adhesion, proliferation and differentiation [1]. By virtue of these promising characteristics, HAM is utilized in several tissue engineering applications [1, 49].

Research on HAM has identified the existence of diverse growth factors, includ-

ing such as basic fibroblast growth factor (bFGF), epidermal growth factor (EGF), transforming growth factor (TGF)-$\alpha$, -$\beta$1, -$\beta$2 and -$\beta$3, keratinocyte growth factor (KGF), KGF receptor (KGFR), hepatocyte growth factor (HGF), HGF receptor (HGFR), vascular endothelial growth factor (VEGF), and platelet-derived growth factor (PDGF) [55]. It is recognized that every one of these growth factors performs intrinsic functions within the context of the wound healing process.

HAM can be prepared or preserved in several forms such as fresh amniotic membrane, a decellularized membrane, cryopreserved membrane, lyophilized or air dried membrane [56], or cross-linked membranes that crosslinked with an appropriate crosslinking agents with an optimal concentrations to enhance mechanical strength and degradation characteristics of HAM [57, 58]. In addition, dried micronized amniotic membranes, amniotic cytokine extracts, and amniotic cytokine extracts as eye drops constitutes another application forms of HAM [2].

### 2.4.1 HAM in Tissue Engineering and Regenerative Medicine Applications

HAM has been utilized in regenerative medicine practices for long years because of its excellent properties like lacking immunogenicity, antifibrotic, anti-inflammatory, anti-angiogenic and antimicrobial features, suitable mechanical properties, and immunomodulatory effects [59]. In addition to its ongoing clinical practices in ophthalmology, dermatology, oral and maxillofacial surgery, it has been deeply examined as a valuable scaffold material for tissue engineering applications.

Acellular HAM has been studied as cell carrier scaffold for several types of cells like epithelial cells, limbal stem cells, differentiated neural-like cells and so many different stem and non-stem cell types [60–63].

To enhance the properties of HAM as well as facilitate its manipulation and augment its durability, numerous modifications were applied. These modifications were summarized as obtaining hydrogels based on HAM, preparing amniotic membrane ex-

tract (AME), amniotic membrane coatings, composites based on HAM, composites containing amniotic membrane particles and composites based on AME [64]. In the study from literature, composite materials were constituted by attaching AM to lyophilized sponge polymeric material. Related cells like skin cells (fibroblasts and keratinocytes) were planted on the AM side of the composites and on conventional scaffolds. It was observed that AM-containing experimental group had anti-inflammatory effect and increased wound healing in animal experiments [65]. In another study AM was anchored to PVA hydrogel and used to improve epithelization of rabbit corneal epithelial cells, according to results this hybrid material promoted stratified epithelial layer and it seemed that epithelial cells feel more like in their natural environment, their morphology and orientation was very similar to native cornea [9]. Another approach is using laminated AM layers to create a tissue equivalent. In related study, ultrathin HAM membrane and corneal stromal cells were utilized to create a corneal stromal tissue equivalent. After seeding keratocyte on ultrathin HAM, membranes were laminated up to four layers and implanted into rabbit corneas with lamellar keratoplasty. *In vivo* examinations showed that this 3D construct provides keratocytes to produce their native ECM, collagen fibers after implantation [49].

Micronized amniotic membrane particles is another application form of amniotic membrane [5]. This form of HAM was added into three dimensional (3D) biomaterials as a bioactive component and its potential effects were investigated in many studies. Hortensius et. al. incorporated dry, homogenized, micronized AM into collagen scaffolds and investigated immunomodulatory effects of AM in adult tendon wound repair. Their results showed that scaffolds including AM matrix have enhanced mechanical properties. In addition, despite the pro-inflammatory cytokine interleukin-1 beta including-growth media, tendon cells that seeded on these AM containing composite scaffolds have higher metabolic activity [66].

Another strategy involves utilizing amniotic membrane extract (AME), which encompasses nearly all the therapeutic constituents present in cryopreserved amniotic membrane (AM) [67]. The effectiveness of HAM and amniotic membrane homogenate or extract (AME) on corneal repair in the rabbit model were compared by Guo *et al.*,

no meaningful difference between the homogenate and membrane group was observed which proves that the effectiveness of amniotic membrane homogenate [15]. AME can be utilized as an eye drop for the therapy of ocular surface disorders, chemical burns or dry eye diseases [6] or by controlled releasing from inside the polymeric nanoparticles (chitosan-dextran nanoparticles) [68] or as a therapeutic agent in polymeric hydrogels (Hyaluronic acid hydrogel) [13]. AME application as an eye drop has several advantages over conventional AM transplantation, like delivering therapeutic substances more extended period without the need for surgical intervention [67].

## 2.5 Artificial Tears

Artificial tears are eye drops used to slicken and retain humidity on the surface of the eyes, helping to alleviate dryness. The U.S. Food and Drug Administration (FDA) classifies artificial tears into two categories: demulcent agents and emollient agents. The ingredients in commercial tear drops can vary significantly. Carboxymethylcellulose sodium, dextran, glycerin, propylene glycol, polyvinyl alcohol, povidone, lanolin, polyethylene glycol are some of the examples of FDA approved tear components [69, 70]. Artificial eye drops, also known as artificial tears, are primarily used to treat a variety of conditions such as Dry Eye Syndrome, allergies, post-surgical recovery or wound healing. Several artificial eye drops were evaluated by Zhang et. al. for their efficacy on corneal epithelial healing in rabbits. Although their effectiveness can vary, all artificial eye drop groups, for instance contained 0.9% normal saline or 0.1% hyaluronate support the re-epithelialization of the cornea [71]. In this thesis, eye drop contained PVA (1.4%) and povidone (0.6%) was used for the experiments.

## 2.6 Exosomes

Extracellular vesicles, characterized by phospholipid bilayer membranes, are actively released by many cell types and contributes significantly to intercellular commu-

nication. These vesicles are present in different physiological fluids, and they are categorized into three subgroups, as exosomes, microvesicles, and apoptotic bodies based on their size, composition, biogenesis, and release mechanism. The size of exosomes varies within the range of approximately 30 to 200 nm [16]. While exosomes' complete physiological functions remain incompletely elucidated, it is thought that they are involved in intercellular signalling to maintain cellular homeostasis and facilitate the elimination of cellular waste products. Exhibiting a composition resembling complex cargo molecules, exosomes encompass a range of cell constitutes, such as DNA, RNA, lipids, metabolites, and both cytosolic and cell-surface proteins. This diverse composition renders exosomes valuable for both diagnostic and therapeutic applications in clinical settings [17]. Exosomes acquired from various cell types like; MSCs , fibroblasts, keratinocytes, macrophages and milk [72]. The process of exosome formation and their molecular cargo were depicted in Figure 2.3.

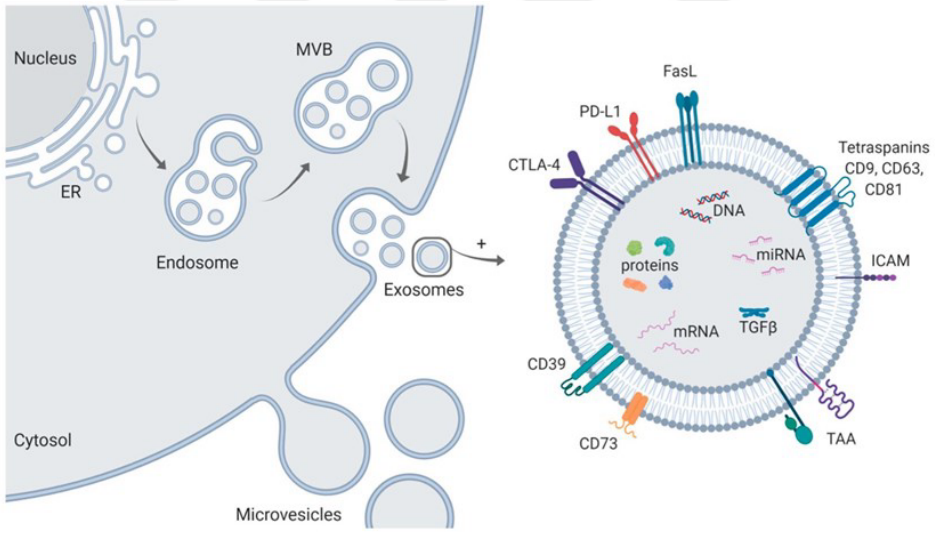


**Figure 2.3** Illustrative depiction of the process of exosome formation and the molecular cargo involved [73].

Classification of exosomes can be based on whether they are subjected to artificial modifications or remain in their natural state. They can be categorized into two subsets: natural and engineered exosomes. The classification of exosomes is summarized in Figure 2.4 adapted from [18].

This classification was performed according to source of exosomes. Adipose de-

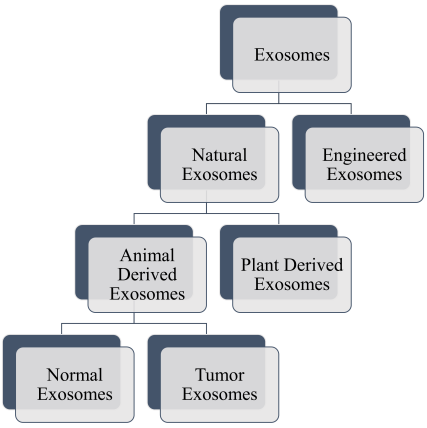


**Figure 2.4** The classification of exosomes based on their source (adapted from)[18].

rived mesenchymal stem cells (AD-MSCs) exosomes [74], exosomes from human cord blood plasma [75] or exosomes obtained from WJ-MSCs [23] can be given as examples of natural exosomes. Engineered exosomes have been designed as drug delivery vehicles for targeted therapies. These exosomes are loaded with drug molecules via several techniques like sonication, electroporation, co-incubation with exosomes, or gene-editing method is used. The primary approach in gene editing method involves employing genetically modified host cells to incorporate the therapeutic agent into the respective exosomes [76]. In addition, surface modifications of exosomes have been performed to precisely target therapeutic drugs [18].

Plant derived exosomes like nanoparticles (PDEN), in other words plant derived exosomes (PLDE) resembles structurally animal or mammalian derived exosomes, but there are some differences in terms of their cellular origin and functions. Ginger, garlic, Shiitake Mushroom, blueberry and grape are different plant sources that used in the studies for therapeutic purposes [77]. In the literature there are many *in vitro*, *in vivo* and few clinical studies that investigated the therapeutic effects of plant exosomes. While PDEN are not as widely recognized as their mammalian counterparts, which have undergone extensive investigation, there is a growing trend in research in this direction [78, 79].

When it comes to animal or mammalian derived exosomes, these exosomes could be present in the cell culture medium of nearly all cell type, and also found in most of body fluid such as blood, saliva, urine, breast milk, amniotic fluids, hydrothoracic fluids, and ascitic fluid [80]. Exosomes are also known with their involvement in regulating the wound healing process through specific signalling pathways [19]. Exosomes from different types of cell sources such as corneal mesenchymal stromal cells, corneal epithelial cells and iPSCs were investigated for their effects on corneal wound healing [20–22]. While iPSCs-Exos exhibit more robust therapeutic effects, both MSCs-Exos and iPSCs-Exos demonstrate the ability to inhibit programmed cell death in human corneal epithelial cells (HCECs) and promote the *in vitro* cell proliferation and migration of HCECs. Additionally, they contribute to *in vivo* wound healing [22]. Exosomes from human cord blood have been utilized for skin wound healing and the results revealed that exosomes demonstrate an effective capability to promote healing of skin wounds by enhancing processes such as angiogenesis, fibroblast proliferation and migration, and the differentiation of M2 macrophages [75].

Another source of exosomes is WJ-MSC. These types of exosomes are obtained from MSCs found in WJ which is a connective tissue found in umbilical cords. These types of MSCs, WJ-MSC, are younger compared to cell found in adipose and bone marrow tissues, making them relatively more protected to aging related damages [23]. In a recent investigation, it was reported that exosomes derived from WJ-MSC (WJ-MSC-Exo) are enhanced keratinocyte growth and migration more effectively than AD-MSCs-exosomes [81]. In another study, proteins in WJ-MSC-Exo cargo were analysed and it was detected that WJ-MSC-Exos have substantial amount alpha-2-macroglobulin proteins. It is stated that this protein may be related with the underlying mechanism of wound healing [82].

# 3. THE EFFECTS OF COMBINED USE OF AMNIOTIC MEMBRANE EXTRACT AND EYE DROP ON CORNEAL KERATOCYTE CELLS (PRELIMINARY STUDIES)

In this part of the thesis, HAM was obtained, stored in appropriate conditions, characterization studies were performed to identify the material. Then HAM was micronized and incorporated into gelatin hydrogels. SEM was employed to characterize obtained biocomposite materials. This part of the thesis could be attributed as preliminary studies. After biocomposites were prepared, it was observed that the micronized particles were not distributed homogeneously within the scaffolds, so it was decided to continue the study by creating an AME, which could distribute the amniotic membrane components more homogeneously. In the following phase of the study, the isolated effects of AME with different concentrations and the effects of using AME with preservative-free eye drop (ED) on corneal keratocyte cells behaviour were examined *in vitro*. The effects of AME with different concentrations and preservative-free eye drop (ED) on cell growth in cultured human corneal keratocytes were investigated. The findings show that combined use of 50 $\mu g$ AME and 4% eye drop increase corneal keratocyte cellular proliferation. Details of each experimental procedure were provided below.

## 3.1 Storage of Fresh Human Amniotic Membrane (HAM)

The HAM provided from Stembio, Cord Blood Cell and Tissue Center, Kocaeli, Turkey, formerly FlorenCell Cell and Tissue Center, Istanbul. Fresh HAM in isotonic solution was fragmented, and a portion of these fragments was preserved at -80 °C in a solution comprising equal parts Dulbecco's Modified Eagle Medium (DMEM) and glycerol (86% in DMEM). This preservation medium included 1% penicillin-streptomycin and 1% gentamicin for future utilization [59]. The preparation steps before freezing the HAM were summed up in Figure 3.1.

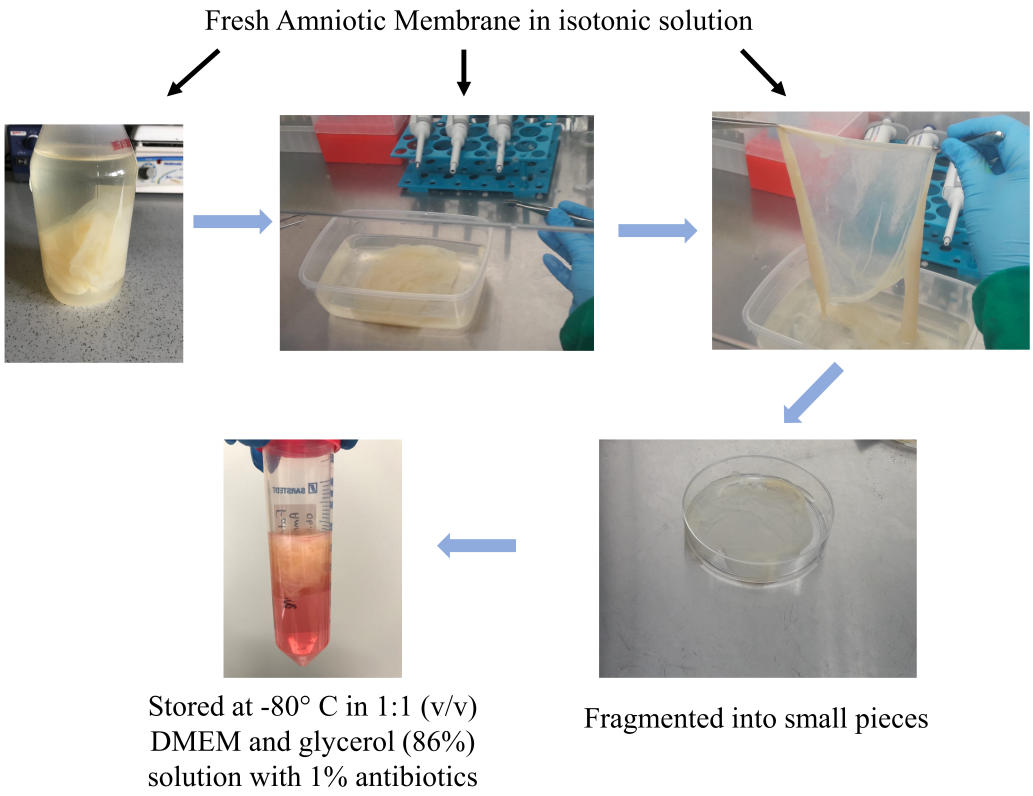


**Figure 3.1** Storage of Fresh Human Amniotic Membrane (HAM).

## 3.2 Characterization and Processing of Fresh Human Amniotic Membrane

### 3.2.1 Scanning Electron Microscopy (SEM) Analysis

SEM analysis of freeze-dried and fixed fresh human amniotic membranes was performed with two different scanning electron microscopes. Firstly, freeze-dried HAM on nitrocellulose paper was examined with SEM (Philips XL30 ESEM-FEG/EDAX) at Advanced Technologies R&D center Laboratory, Boğaziçi University. Then fresh HAM were investigated with Quattro S (ThermoFisher Scientific) at Boğaziçi University Life Sciences and Technologies Application and Research Center. Image of fresh HAM before these characterization studies was shown in Figure 3.2.

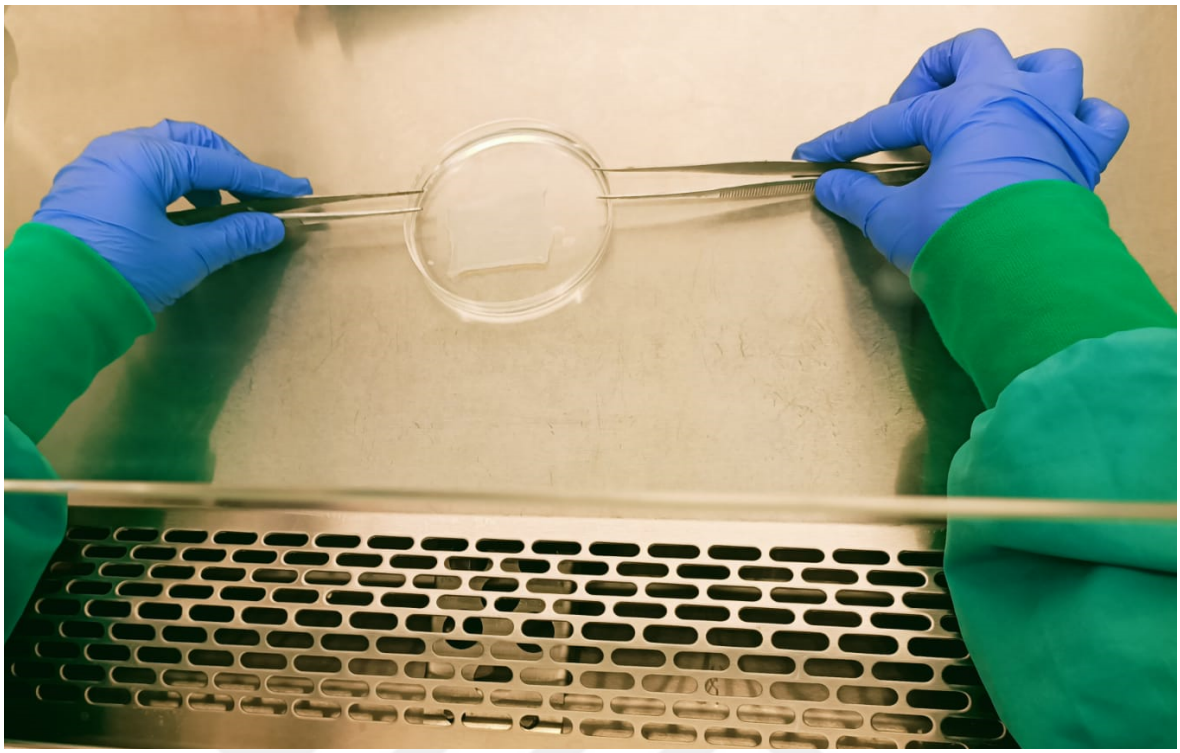

**Figure 3.2** Fresh HAM before characterization studies.

Fresh HAM sections were preserved using 4% paraformaldehyde in a 0.1 M phosphate buffer solution (pH 7.4) for 2 hours at ambient temperature. After rinsing with Phosphate Buffered Saline (PBS), incubated with 8% formaldehyde for 2 days at 4 °C. The sample was washed again in PBS and then dehydrated using a series of alcohol concentrations: 30%, 50%, 70%, 80%, 90%, and 100% (twice). A HAM pieces was kept in each solution for 10 min. Lastly, incubated in Hexamethyldisilazane (HMDS) solution for 10 min and allowed to dry in open air in hood overnight [83]. SEM images of this fixed fresh HAM piece were obtained with Quattro S (ThermoFisher Scientific) and shown in Figure 3.5.

### 3.2.2 Hematoxylin and eosin (HE) staining

Fresh HAM pieces were kept waiting in 10% formalin solution for a week for fixation. Then this tissue pieces were processed in automatic tissue processor for 24 hours.

Tissue was encased in paraffin with the paraffin entrenched system (Leica EG1150, Leica Microsystems, Germany) and sectioned at 8 um thickness using microtome (RM 2255, Leica Microsystems, Germany). The sections of HAM were stained by haematoxylin and eosin (HE) and examined with a phase-contrast microscope (Nicon, Eclipse 80i). Following recipe was used for HE staining. Sections were submerged in to 100% alcohol for 2 minutes, 90% alcohol for 2 minutes and they were washed in tap water. Then they were dipped into Haematoxylin solution for 1 min, washed in tap water. Following step, they were dipped in alcohol 70%+HCL for 1 min, 80% alcohol for 1 min, 90% alcohol for 1 min, eosin solution for 1 min. After washing with tap water, again sections were submerged into, 90% alcohol for 2 min, 100% alcohol for 2 minutes, xylene for 5 dips, respectively. The samples were dried for 30 seconds and then coated with entellan.

## 3.3 Preparation and Characterization of Gelatin-HAM Biocomposite Hydrogels

Micronized amniotic membrane particles is another application form of amniotic membranes. One of our objectives was to develop biodegradable polymeric biocomposites incorporating micronized human amniotic membrane (mHAM), with the intention of application in corneal wound healing. HAM was cryogenically pulverized into micron-sized particles using liquid nitrogen. Biocomposite gelatin hydrogels were formulated by incorporating these micron-sized HAM particles, and following their fabrication, the hydrogels underwent lyophilization. Subsequent scanning electron microscopy (SEM) imaging was conducted. To this end, first and foremost, HAM pieces were submerged in liquid nitrogen and crushed in mortar. When samples remove from liquid nitrogen, they become soft and jelly. It was very difficult to separate the samples from the container. So, both the crushed HAM and fresh HAM pieces were freeze-dried. After freeze-drying process, micronized HAM powder was weighted to add into gelatin hydrogel solution. Aqueous gelatin solution was chemically cross-linked with glutaraldehyde (GA) to prepare gelatin hydrogels. 3% gelatin and 0.16% GA were used

for the experiments [84].

Two experimental groups were prepared for biocomposites, gelatin: HAM ratio was 3:1 w/w at first group and was 5:1 at second group. These group were named as Gel1 and Gel2. These ratios were determined because of the high collagen content of AM based on the literature [66]. The solutions contained gelatin, GA and HAM were put into 6-well plates and kept waiting at 4 °C for 12h for crosslinking reaction. Next day, 0.1 M aqueous glycine solution was poured onto gels to immobilize the unreacted aldehyde groups of glutaraldehyde and kept waiting at 37 °C for one hour. Hydrogels were washed with ultra-pure water three times. Then gels were removed to -20 °C. Hydrogels were placed in a freeze-dryer and after freezing lyophilized for 24h (Freeze drying parameters, temperature: -80 °C and chamber pressure: 0.001 millibar) [84].

## 3.4 Preparation of AME

HAM was acquired in a fresh state and immersed in an isotonic solution. These HAM pieces, each measuring 5x5 cm, were subsequently preserved at -80 °C. They were stored in a solution consisting of a 1:1 volume ratio of DMEM and 86% glycerol, which also included 1% penicillin-streptomycin and 1% gentamicin until needed for use [59, 85]. hAM tissue pieces were thawed and cleansed with PBS in three cycles before the micronization process. The procedure for obtaining AME was adapted from a previous study [13]. Tissue pieces were freeze-dried for 24 hours and then micronized until they became a fine powder in the presence of liquid nitrogen with a mortar and a pestle. 220 mg of micronized HAM was weighed, and 22 mg of pepsin was incorporated into this powder. 10 mL of 0.01 N HCl was put into the mixture and the solution was hold at 37 °C for 48 hours. The incubated mixture was then centrifuged at 4100 rpm for 10 minutes and its supernatant was transferred into a different container and neutralized with 0.1 M NaOH. The resulting liquid was aliquoted into 1 mL vials and stored at -80 °C until use. Preparation of amniotic membrane extract was summarized in Figure 3.3.

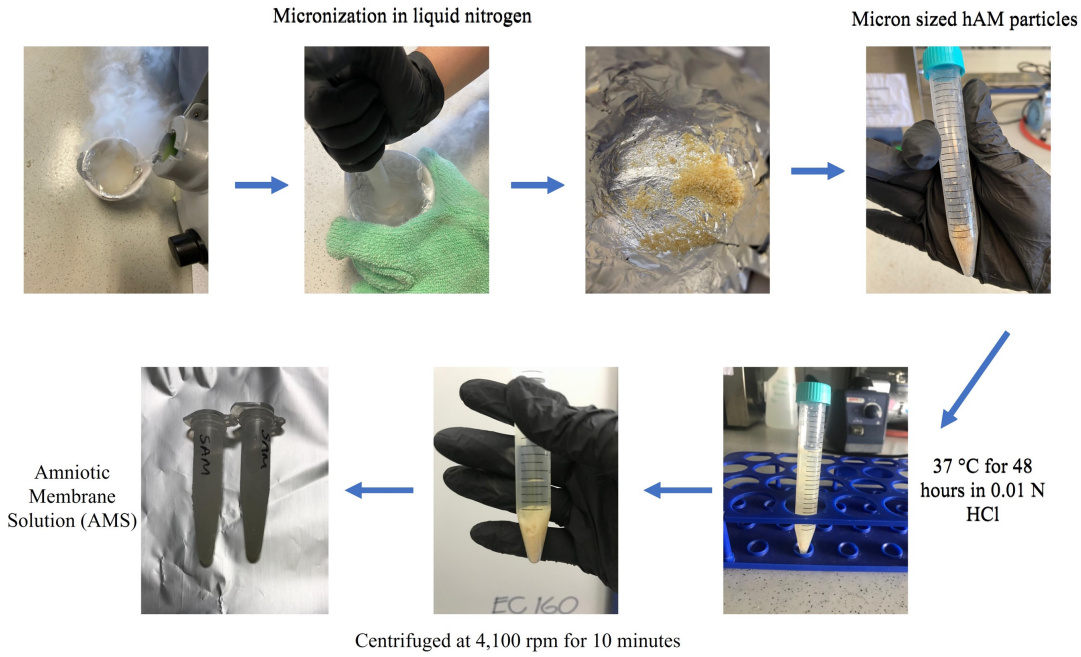


**Figure 3.3** Preparation of Amniotic Membrane Extract (AME) solution.

## 3.5 Characterization of AME

Pierce™ BCA Protein Assay was carried out to identify the total protein amount in amniotic membrane extracts (AME) which obtained from different amniotic membrane pieces. To prevent batch-to-batch differences in protein concentration, the protein content of each AME aliquot was found out via Pierce™ BCA Protein Assay before using. 25 $\mu L$ of samples from each group were added to 200 $\mu L$ of working solution that containing kit reagents. The measurement was performed by applying the manufacturers' protocol. A standard curve was plotted to find out the concentration of unidentified samples. Protein concentrations of AME aliquots were determined using this standard curve.

## 3.6 Cytocompatibility of AME and Combined Use of AME and Eye Drop

The compatibility of amniotic membrane extract (AME) and a preservative-free commercial eye drop with corneal keratocytes was assessed through the use of 3-[4,5-dimethylthiazol-2-yl]-2,5-diphenyltetrazolium bromide (MTT) assay. Human corneal keratocyte cell line (HK P10872, Innoprot) was employed as a cell model for the experiments. 3x$10^4$ cells/well were cultured on 24-well cell culture plates and kept at 37 °C, 5% $CO_2$. DMEM-F12 (Capricorn Scientific) used as cell culturing medium. 10% v/v fetal bovine serum (FBS, Merck) and 1% v/v penicillin/streptomycin (Biosera) were added into this growth medium. As an experimental groups AME solution with various concentrations 50 $\mu g$/mL, 100 $\mu g$/mL, 500 $\mu g$/mL, eyedrops with different dilutions like 1:2 diluted, 1:10 diluted, 1:20 diluted, and mixture group that contains 50 $\mu g$/mL AME + 4% eyedrop (equal volume of AME and Eyedrop) were implemented to corneal keratocytes 24 hours following cell seeding. The viability of the cells was assessed via MTT assay at $1^{st}$ and $2^{nd}$ day of application.

5 mg/mL (in PBS) MTT solution was made ready just before the experiment. This solution was filtered in a laminar cabin with a 0.22 $\mu m$ filter. 40 $\mu L$ MTT solution was put into each well and waited for 3 and a half hours. After removing the medium containing the MTT solution, Dimethyl Sulfoxide (DMSO) was put into each well. The optical density of formazan crystals dissolved in DMSO was measured at 570 nm to determine cell viability. 750 nm served as the reference wavelength. The measurements were performed using a Microplate Reader Spectrophotometer (BIO-RAD iMark).

## 3.7 Findings of the Preliminary Experiments

### 3.7.1 Characterization Results of Human Amniotic Membrane

Cross-sectional SEM images of lyophilized HAM on nitrocellulose membrane, which were obtained via Philips XL30 ESEM-FEG/EDAX, was shown in Figure 3.4. Figure 3.4A demonstrates cross-sectional view of lyophilized HAM on nitrocellulose membrane at 1000X magnification. Figure 3.4B shows the spongy layer of HAM at a higher magnification.

Lyophilisation process can cause shrinkage or collapse of structures, so non-lyophilized HAM membranes were also characterized. SEM images of fresh HAM were taken via SEM (Quattro S, ThermoFisher Scientific) and shown in Figure 3.5. There were no cells on the membrane and organized collagen fibers could be seen with two different magnifications in Figure 3.5 A and B.

HAM sections that were stained by haematoxylin and eosin (HE) were demonstrated in Figure 3.6. As observed in Figure 3.6, microarchitecture of HAM, its layers, extracellular matrix, and other basic components were stained with eosin as different shades of pink. Cell nuclei should be stained with blue or purple. There is no thin layer of epithelial cells on the membrane. Although no protocol was applied to decellularize the membrane, it is thought that the cells on the membrane may have died because it had to be kept for a while for analysis.

### 3.7.2 SEM Characterization Results of Gelatin-HAM Biocomposites

First SEM analysis was performed to observe pore distribution and pore size of gelatin hydrogels. Cross-sectional SEM images of pure gelatin hydrogels and pore sizes were shown in Figure 3.7. Average pore diameters of gelatin sponges were 302,90 $\mu m$.

Sectional view SEM images of Gelatin-HAM Biocomposites (3:1 Gelatin:HAM

ratio) were shown in Figure 3.8. Cross-sectional SEM images of Gelatin-HAM Biocomposites (5:1 Gelatin:HAM ratio) were demonstrated in Figure 3.9.

HAM pieces located in pores of biocomposites can be observed in Figure 3.8 and Figure 3.9. The outcomes show us that the presence of HAM in the biocomposite can be proven via SEM analysis. However, HAM distribution in the composites were not homogenous, since micronized AM pieces became soft and aggregated when they added into hydrogel solution. Therefore, it is decided to continue the experiments with another form of HAM, AME.

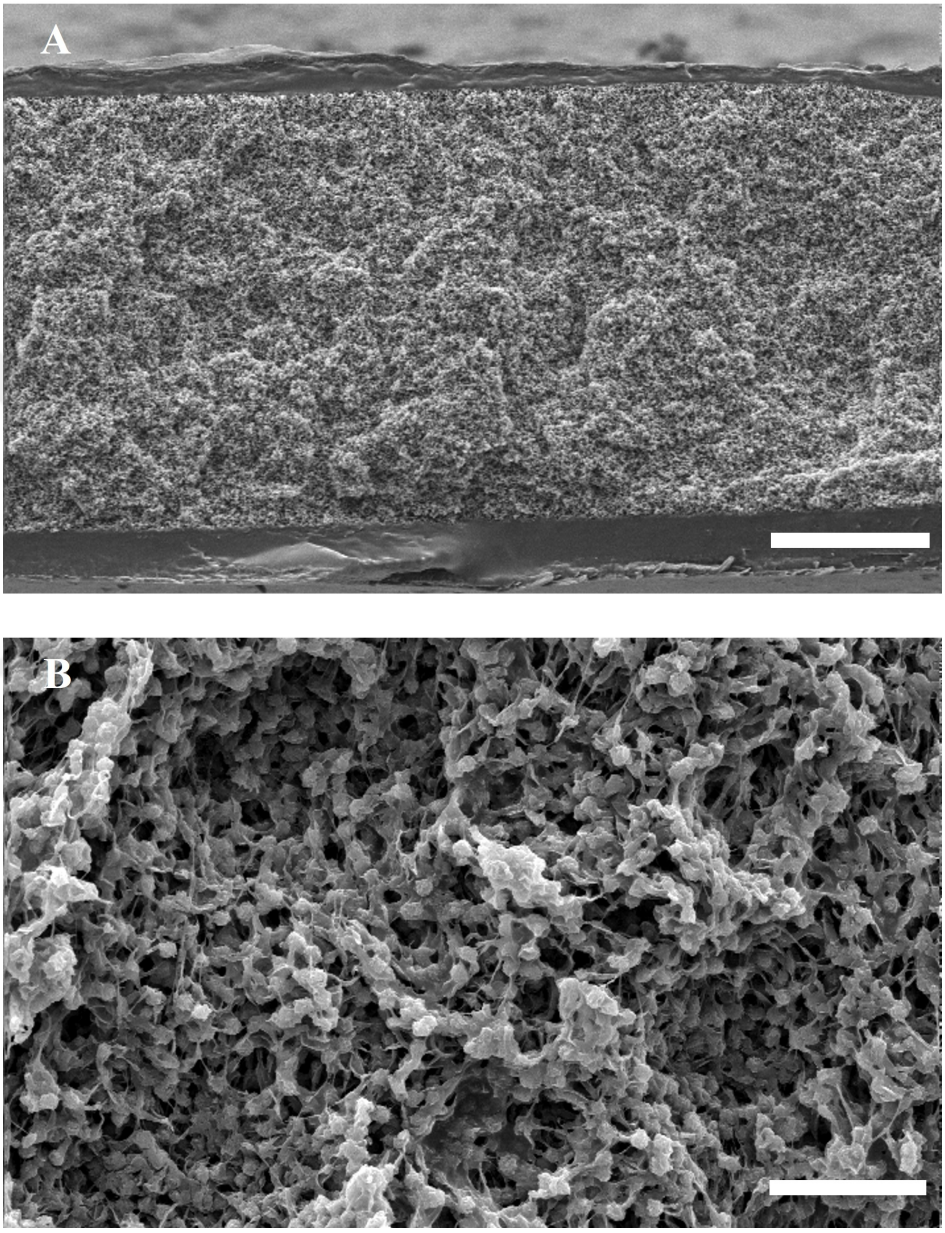


**Figure 3.4** Cross-sectional SEM images of lyophilized HAM. Scale bar: 50 $\mu m$(A), 5 $\mu m$ (B).

### 3.7.3 Characterization of AME

Total protein amount in amniotic membrane extract was determined as 1.2 mg/mL, 1.3 mg/mL and 1.4 mg/mL from different piece of HAM, respectively. Based on this concentration data, several experiments were designed with corneal keratocytes to evaluate cytocompatibility of AME.

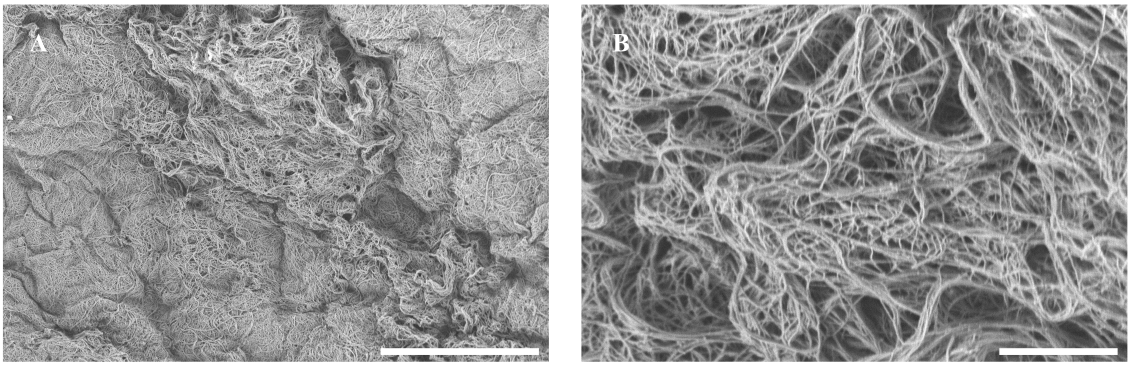


**Figure 3.5** SEM images of fresh Human Amniotic Membrane. Scale Bar: 30 $\mu m$ and 3 $\mu m$ respectively.

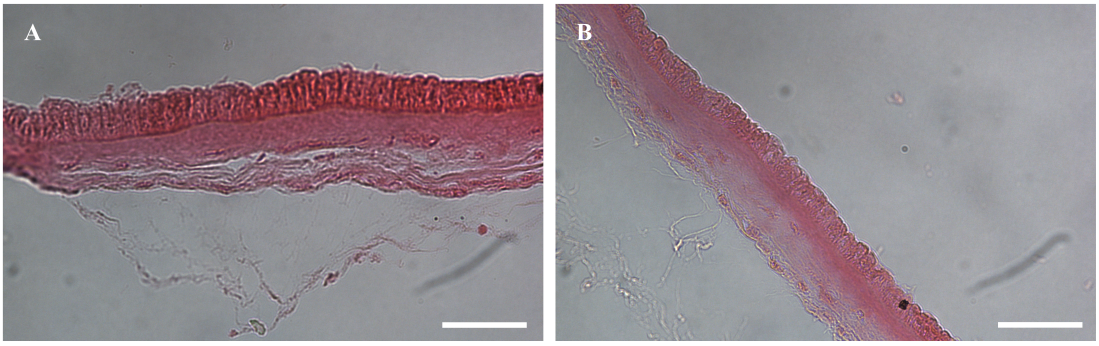


**Figure 3.6** Haematoxylin-Eosin Staining of Human Amniotic Membrane. Scale bar 10 $\mu m$ (A), 10 $\mu m$(B).

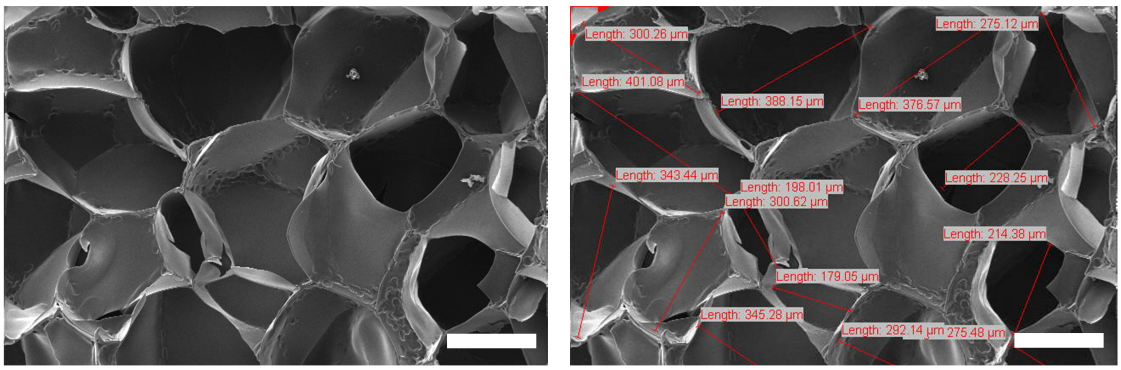


**Figure 3.7** Cross-sectional SEM images of gelatin sponge and pore sizes.

### 3.7.4 Cytocompatibility of AME and Combined Use of AME and Eye Drop

MTT assay results after application of different concentrations of eye drops and combined used with AME were shown in Figure 3.10. Application of 50 $\mu g$/mL AME increases corneal keratocyte cell proliferation two days after application ($p < 0.0001$). The comparison of 50 $\mu g$/mL AME and 100 $\mu g$/mL AME concentration in terms of cell viability revealed no significant statistical difference. In addition, excessive increase in AME concentration (500 $\mu g$/mL) caused cell viability to decrease.

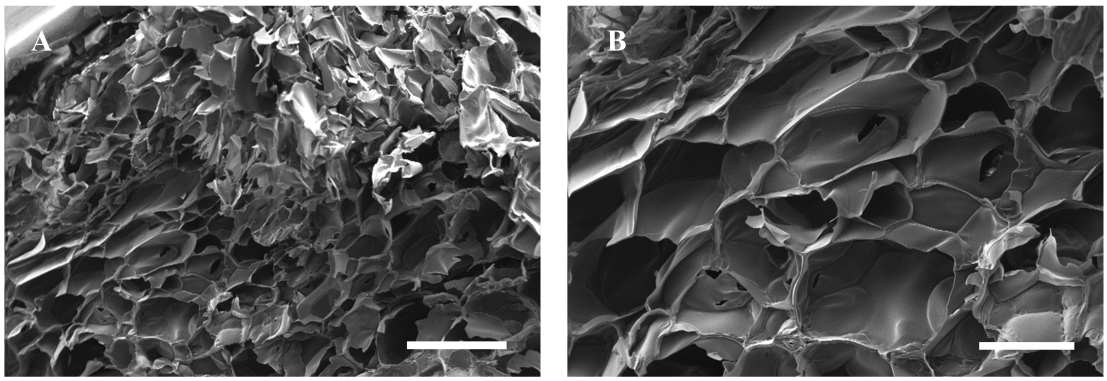


**Figure 3.8** Cross-sectional SEM images of Gelatin-HAM Biocomposite (3:1 Gelatin:HAM ratio) Scale bar 500 $\mu m$(A), 200 $\mu m$(B).

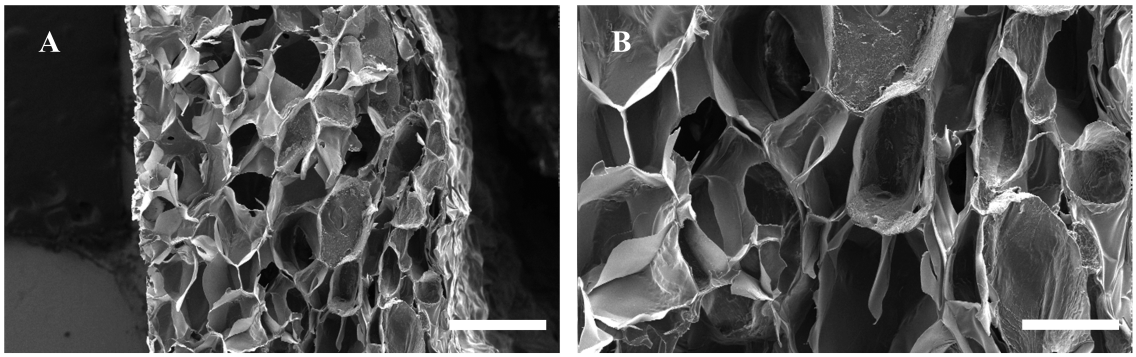


**Figure 3.9** Cross-sectional SEM images of Gelatin-HAM Biocomposite (5:1 Gelatin:HAM ratio). Scale bar 500 $\mu m$(A), 200 $\mu m$(B).

Combined use of 50 $\mu g$/mL AME and 4% eye drop increases cell viability significantly compared to only 1:20 diluted eye drops application ($p<0.0001$) and compared to only 50 $\mu g$/mL AME ($p<0.0001$).

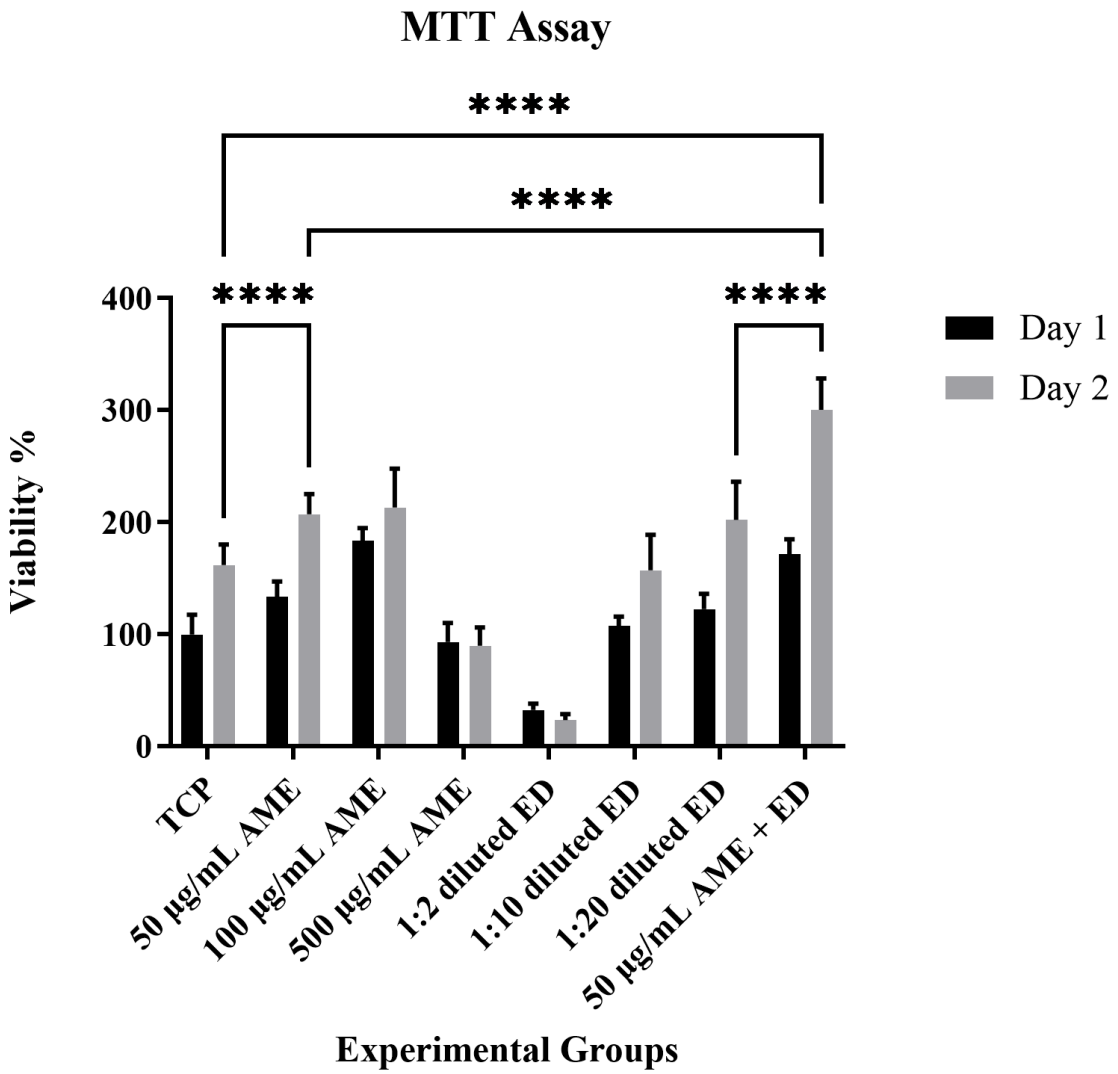


**Figure 3.10** MTT Assay Results 1 and 2 days after AME and Eye Drop Application.

## 3.8 Discussion

In the initial phase of the thesis, first efforts were centered on the characterization of HAM. Morphological characterization was performed with two different SEM devices for both lyophilized and fresh HAM. After characterization studies of fresh and lyophilized HAM, HAM was micronized to obtain micron-sized HAM particles. Micron-sized HAM particles were incorporated gelatin biocomposites. However, it was observed

that a totally homogeneous distribution could not be achieved with this method. Therefore, in the later stage of the study, it was decided to use extract form of HAM (AME) to obtain more uniform dispersion. AME was prepared and the cytocompatibility of AME with different concentration was evaluated. 50 $\mu g$/mL AME increases corneal keratocyte cell viability in comparison to TCP ($p<0.0001$). There was no notable statistical difference between 50 $\mu g$/mL AME and 100 $\mu g$/mL AME application, so 50 $\mu g$/mL AME concentration was chosen for the following experiments. Subsequently, an investigation was conducted to assess the impact of employing AME with preservative-free eye drop on corneal keratocyte behaviour. A commercial preservative-free eye drop contained PVA (1.4%) and povidone (0.6%) was used for the cell culture experiments. Combined use of 50 $\mu g$/mL AME and 4% eye drop increases corneal keratocyte cell viability compared to 1:20 diluted eye drop application ($p<0.0001$), only 50 $\mu g$/mL AME application ($p<0.0001$) and compared to TCP ($p<0.0001$).

Artificial eye drops have been used for corneal healing for many years. Artificial tears contain salt, water, and many different ingredients like PVA, hyaluronic acid (HA), polyethylene glycol, carboxymethyl cellulose. In the investigation conducted by Zhang *et al.*, the effects of different eye drops on corneal re-epithelization were evaluated and it was reported that all manufactured eye drops performed superior to the control group and enhanced corneal re-epithelium [71]. Because of these favourable effects, artificial eye drops have been utilized prevalently for corneal wounds.

AME has been also utilised as in an eye drop form (AMEED) for acute or chronic chemical burns, acute corneal injury, and corneal epithelial wound studies [6]. It has been reported that AMEED possesses many similar properties to cryopreserved AM, such as a high concentration of growth factors. These growth factors have been shown to successfully pass through the cornea in ex vivo studies [86].

In this thesis, the outcomes revealed a discernible augmentation in cellular proliferation upon concurrent administration of AME and eye drop. This result may be arisen from the PVA content of the eye drops in addition to the growth factors in AME. In the literature, hyaluronic acid (HA) is more often utilized in combination

with other components in artificial tears to increase epithelial cellular proliferation and wound healing [87]. PVA containing artificial tears perform a supporting role in corneal wound healing via providing moisture and lubrication. There is less documented information about the direct enhancing effects of PVA on cell proliferation compared to HA. However in the literature, addition of PVA in a growth medium (1 mg/mL) promoted the growth of human pluripotent stem cells in suspension culture [88]. In another study, PVA/collagen composite nanofibrous electrospun scaffolds promote the proliferation and adhesion of the HCECs and keratocytes [89].

As far as it is known, there is no study about the combined use of AME and PVA containing eye drops for corneal regeneration. However, additional research is necessary to validate the benefits of combined use of AME and PVA containing eye drops on corneal keratocytes proliferation.

# 4. MESENCHYMAL STEM CELLS DERIVED-EXOSOMES ENHANCED AMNIOTIC MEMBRANE EXTRACT PROMOTES CORNEAL KERATOCYTE PROLIFERATION

In this part of the study, AME and WJ-MSC-Exos used together to investigate their effects on corneal keratocytes behaviour. While both WJ-MSC-Exos and AME have been individually utilized in wound healing research, their combined synergistic effects have not been studied extensively. Following characterization studies of both AME and WJ-MSC-Exos, the effects of both AME and WJ-MSC-Exos, individually and together, on the proliferation of corneal keratocytes as well as their ability to promote *in vitro* cell migration, wound healing, and their impact on cellular morphology were evaluated. Our results shows that presence of both exosomes and AME synergistically enhance the proliferation of corneal keratocytes. The simultaneous application of these remedies has proven to enhance the rate of wound closure when contrasted with the exclusive use of WJ-MSC-Exos. The overall efficacy of employing a combination of AME and exosomes in wound healing applications, along with its positive influence on bolstering cell proliferation, can strengthen the current methodologies employed in corneal repair research.

All experimental procedures for this part of the thesis were summarized in Figure 4.1.

## 4.1 Preparation and Characterization of AME

AME was prepared based on the protocol, which is given the section 3.4. Then the total protein amount in AME solutions was determined by using Pierce™ BCA Protein Assay Kit (ThermoScientific, USA) as per the manufacturer's guidelines. Bovine serum albumin (BSA) standards were prepared with final concentrations of 2000 $\mu g$/mL, 1500 $\mu g$/mL, 1000 $\mu g$/mL, 750 $\mu g$/mL, 500 $\mu g$/mL, 250 $\mu g$/mL, 125 $\mu g$/mL, 25 $\mu g$/mL. Reagents were added into each standard and unknown AME sample, and their ab-

sorbances were measured at 570 nm in a microplate absorbance reader (Bio-Rad, iMark, USA). After subtraction of blank standard measurements at 570 nm, a calibration curve was plotted, and the protein content of AME samples were determined. Calibration curve for Pierce BCA Protein Assay for second batch of AME aliquots was given in Figure A.1.

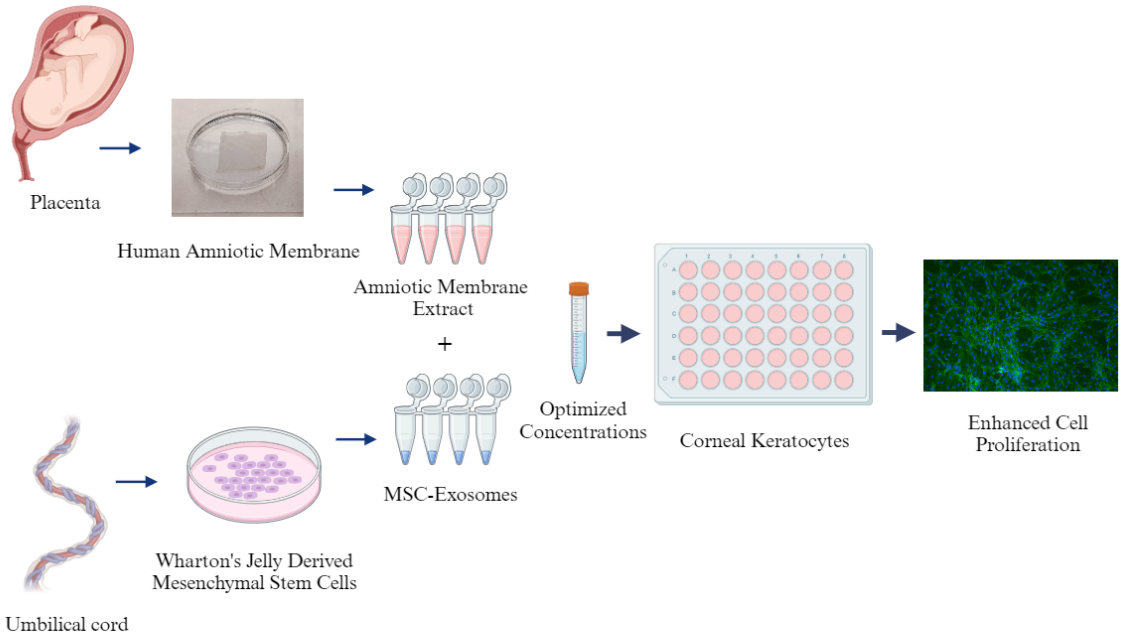


**Figure 4.1** Graphical abstract of experimental procedures. In this part of the study AME have been combined with WJ-MSC-Exos. Corneal keratocyte behavior was observed to be enhanced after optimization of mixture concentrations. Created with BioRender.com

## 4.2 Characterization of WJ-MSC-Exos

WJ-MSC-Exos are denoted as Exo throughout the study. WJ-MSC-Exos with a concentration of 1.25x$10^9$ particles/mL were obtained from a tissue/blood bank (Stembio, Cord Blood Cell and Tissue Center, Kocaeli, Turkey). This suspension was thawed once to divide into 50 $\mu$L aliquots and kept at -80°C until subsequent use. All further use and characterizations were performed immediately after thawing the aliquots.

### 4.2.1 Dynamic Light Scattering (DLS) Measurements for Exo

Zetasizer Advance Series-Pro Blue Label (Malvern Panalytical, UK) was utilised to determine the size distribution and polydispersity of the exosomes. 10 $\mu$L of Exo suspensions were diluted with a ratio of 1:100 with PBS to obtain a 1000 $\mu$L final suspension and transferred into a cuvette and measured. For each sample, three scattering measurements were performed to assess size and density, and the average size and polydispersity index (PDI) of the exosomes were acquired.

### 4.2.2 Scanning Electron Microscopy Analysis of Exo

Quattro Environmental Scanning Electron Microscope (ESEM, Quattro S, Thermo Fisher Scientific, US) was used for morphological characterization of Exo. 10 $\mu$L of exosome suspension was dropped onto the grid and analyzed using a STEM 3 detector. The images were captured at an electron beam voltage of 30 kV and a spot size of 1.0. The working distance was kept at 6.9 mm.

## 4.3 Cytocompatibility of AME and Exo

### 4.3.1 MTT assay

Cell culture studies were carried out with L929 fibroblast cells and corneal keratocytes. The non-cytotoxic AME concentration range was determined using L929 fibroblast (American Type of Culture Collection (ATCC), CCL-1) cells. 3x10$^4$ cells/well were plated onto 24-well cell culture plates and incubated at 37°C, 5% $CO_2$. DMEM high glucose (4.5g/L) supplemented with L-glutamine and sodium pyruvate utilised as cell culture medium. 10% v/v FBS, and 1% v/v penicillin/streptomycin were added into this growth medium. AME solutions at different dilutions of 700 $\mu g$/mL, 280 $\mu g$/mL, 140 $\mu g$/mL, 70 $\mu g$/mL, 28 $\mu g$/mL, and 14 $\mu g$/mL were applied to the cells 24 hours after cell seeding. The MTT assay was conducted to evaluate cell viability 48

hours following application.

### 4.3.2 alamarBlue Cell Proliferation Assay

alamarBlue cell proliferation assay was performed to evaluate the effects of AME and Exos on corneal keratocyte proliferation. Human keratocytes obtained from collagen lamellae in the corneal stroma (Innoprot, Spain P10872) were used for cell culture experiments. 1x104 corneal keratocytes/well were seeded into 48-well plates. 3x$10^5$ Exo/mL, 50 $\mu g$/mL AME, and 3x$10^5$ Exo/mL + 50 $\mu g$/mL AME treatments were applied to cells after 24 hours of initial cell seeding. Serum-free medium (DMEM-F12, Capricorn Scientific) was used to dilute AME and exosome solutions and used as vehicle control to specifically observe the effects of AME and exosomes without possible interferences from proteins found in FBS. alamarBlue assay was performed after 24 hours, 48 hours, and 72 hours, following AME and Exo applications. 10% alamarBlue solution (Invitrogen, ThermoFisher Scientific, USA) in growth medium was put into each well and incubated at 37°C for 3.5 hours. After incubation, 100 $\mu L$ of the solution from each well was conveyed to a 96-well plate. Absorbance values were measured at 570 nm and 595 nm with a microplate reader (Bio-Rad, iMark, USA).

## 4.4 Actin Cytoskeleton and Nuclei Staining

Cellular morphologies of adherent corneal keratocytes following AME and Exo treatments after 2nd day of cell culture were investigated with actin cytoskeleton staining. First, adherent cells were rinsed with PBS twice. 4% paraformaldehyde was utilised for the fixation protocol (for 15 minutes). Then 0.1% Triton-X 100 (in PBS) was put into wells for permeabilization. After waiting 5 minutes in permeabilization solution and rinsing. 1% bovine serum albumin (BSA) in PBST were added onto adherent cells for blocking and waited for 30 minutes. 0.015% v/v conjugated phalloidin in 1% BSA solution was put into each well for 20 minutes and counterstained with DAPI for 3 minutes. Cells were rinsed with PBS twice and observed under a fluorescent mi-

croscope (DM IL, Leica, Germany) with their respective filters (green excitation (488 nm) for phalloidin and blue excitation (365 nm) for DAPI) (DM IL, Leica, Germany).

## 4.5 *In Vitro* Scratch Assay/ Cell Migration Assay

Wound healing potential of AME and Exo concentrations were investigated with an *in vitro* scratch assay. Corneal keratocytes were seeded on 24-well culture plates with a seeding density of 5x$10^4$ cells per well. When cells have reached confluency, a wound was created with a sterile 200 $\mu L$ micropipette tip by scratching from top to bottom of each well. The detached cells were removed by two rounds of rinsing with PBS. Assay protocol was adapted from [90]. 50 $\mu g$/mL AME, 3x$10^5$ Exo/mL and 50 $\mu g$/mL AME + 3x$10^5$ Exo/mL treatments were applied to cells and incubated for 24 hours at 37°C in an 5% $CO_2$ incubator. Cells were imaged under an inverted optical microscope (DM IL, Leica). To quantify of the wound closure ratio (%), images were binarized on GIMP (GNU Image Manipulation Program) and white and black pixels were counted in ImageJ (National Institutes of Health, USA). The wound closure ratio was calculated as the percent reduction in wound area after 24 hours.

## 4.6 Statistical Analysis

All findings were reported as the mean ± standard deviation. Differences among means of measurements between experimental groups were determined with ordinary one-way ANOVA test. Tukey's post-hoc analysis following a two-way ANOVA test was used for grouped sample analysis. $p<0.05$ was regarded as statistically significant. Statistical significance was represented by * for $p<0.05$, ** for $p<0.01$, *** for $p<0.001$ and **** for $p<0.0001$.

## 4.7 Results

### 4.7.1 Characterization of AME

To prevent batch-to-batch differences in protein concentration during experiments, the protein content of each AME aliquot was measured individually before use. Total protein amounts in AME aliquots obtained from HAM were calculated as 1.6 mg/mL, 1.8 mg/mL, and 1.4 mg/mL by using AME calibration curve (Figure A.1).

### 4.7.2 Characterization of Exo

Exo were also characterized before cell culture experiments. Three scattering measurings for size and density were captured for each sample during dynamic light scattering (DLS) measurement. The mean hydrodynamic size of the sample was measured as 152.8 nm ± 7.701 nm, polydispersity index (PDI) of the sample was 0.457 ± 0.1031.

DLS results demonstrating the particle size distribution by number % and intensity % (Figure 4.2, A and B). SEM imaging has revealed that exosomes have a round morphology, and their sizes were measured as 166.73 nm ± 40.35 nm, supporting the data from DLS results (Figure 4.2, C).

### 4.7.3 Cytocompatibility of AME and Exo

#### 4.7.3.1 MTT Assay

MTT assay was carried out to detect potential cytotoxicity of different doses of AME on L929 fibroblast cells and to find an optimum range for AME concentrations to be used in further cell culturing (Figure 4.3). Changes in cell viabilities after treatment with AME concentrations of 140 $\mu g$/mL, 70 $\mu g$/mL, and 28 $\mu g$/mL were not

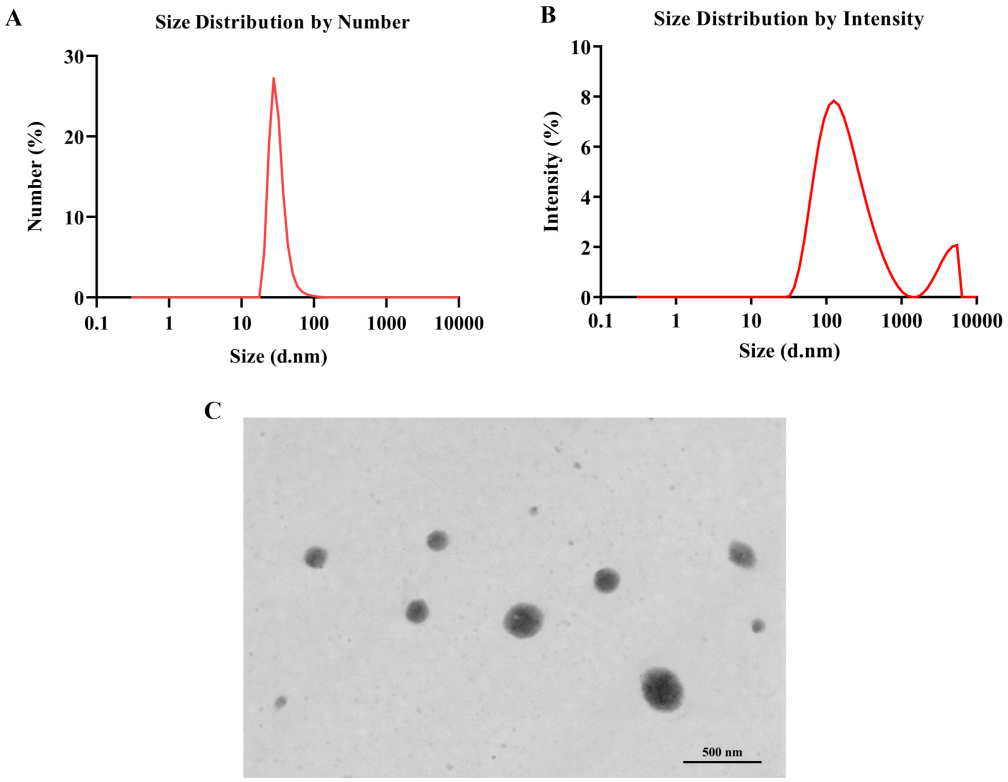


**Figure 4.2** Characterization of WJ-MSC-Exos. A) DLS measurement for Exo size distribution by number %, B) DLS measurement for Exo size distribution by intensity %, C) SEM image of WJ-MSC-Exos (Scale bar: 500 nm).

statistically meaningful (ns: $p \geq 0.05$).

#### 4.7.3.2 alamarBlue Assay

Two different exosome concentrations ($3x10^5$ Exo/mL and $3x10^6$ Exo/mL) were assessed for cell proliferation using alamarBlue assay on day 1, day 2, and day 3 (Figure 4.4 A). There was no statistically significant difference in cell proliferation between the two exosome concentrations ($3x10^5$ Exo/mL and $3x10^6$ Exo/mL) on both day 2 and day 3. Consequently, $3x10^5$ Exo/mL was picked out as the working concentration for its individual use and its combination with AME on cell culture studies. Corneal keratocytes treated with vehicle control, $3x10^5$ Exo/mL, 50 $\mu g$/mL AME, and $3x10^5$ Exo/mL + 50 $\mu g$/mL AME were compared to each other with alamarBlue cell proliferation assay on day 1, day 2, and day 3 (Figure 4.4 B).

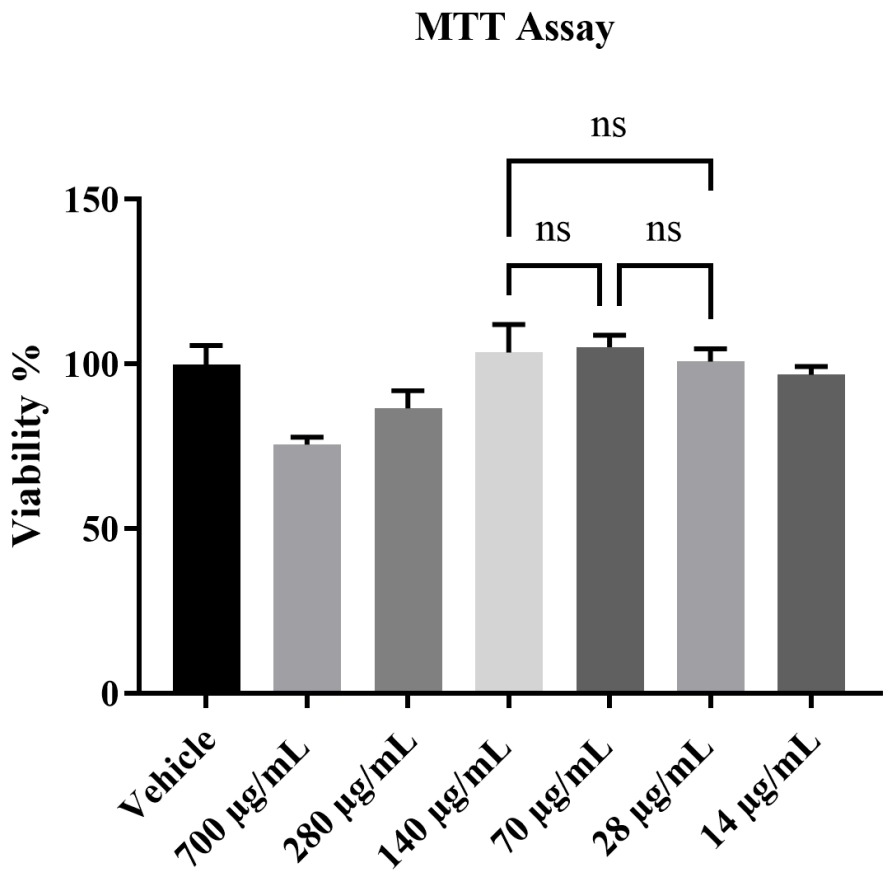


**Figure 4.3** Results of MTT assay on L929 fibroblast cells treated with 700 $\mu g$/mL, 280 $\mu g$/mL, 140 $\mu g$/mL, 70 $\mu g$/mL, and 28 $\mu g$/mL, 14 $\mu g$/mL AME after 48 hours. (ns: $p \geq 0.05$).

Cells treated with $3x10^5$ Exo/mL and with $3x10^5$ Exo/mL + 50 $\mu g$/mL AME resulted in significantly different measurements on both day 2 and on day 3; where, mixture treatment ($3x10^5$ Exo/mL + 50 $\mu g$/mL AME) was significantly higher in cell proliferation (**** $p<0.0001$). Moreover, mixture treatment has significantly higher cell proliferation compared to 50 $\mu g$/mL AME treatment on day 3 (**** $p<0.0001$).

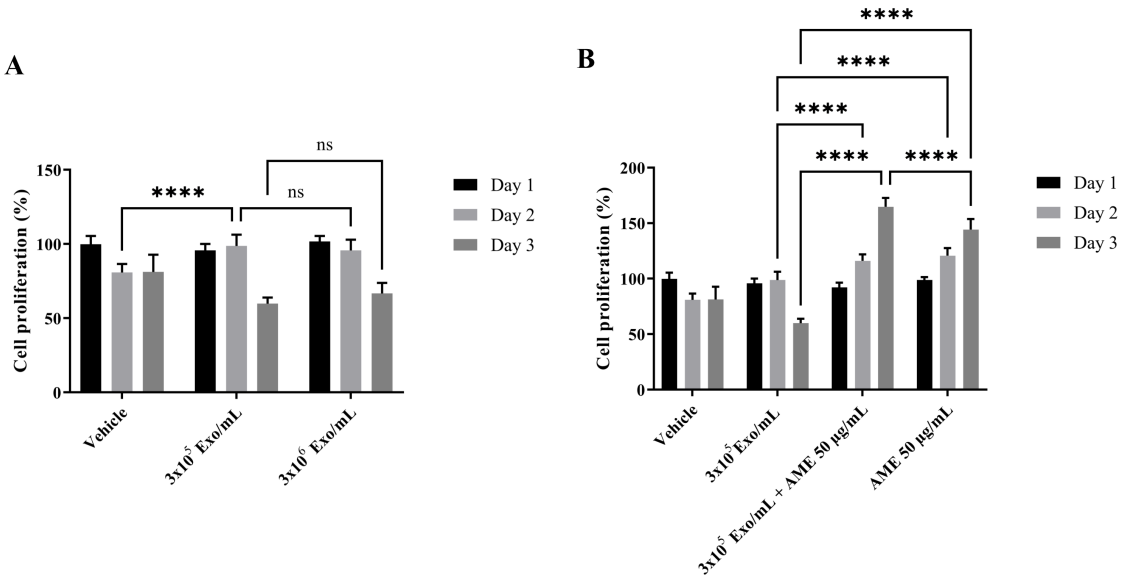


**Figure 4.4** Cell proliferation results for corneal keratocytes, assessed by alamarBlue assay. A) Cell proliferation of corneal keratocytes treated with $3x10^5$ Exo/mL and $3x10^6$ Exo/mL (days 1, 2, and 3). B) Cell proliferation of corneal keratocytes treated with $3x10^5$, 50 $\mu g$/mL AME and 50 $\mu g$/mL AME + $3x10^5$ Exo/mL (days 1, 2, and 3). (ns: $p \geq 0.05$, ****: $p < 0.0001$). Cell proliferations are normalized to day 1 vehicle control.

### 4.7.4 Actin Cytoskeleton and Nuclei Staining (Phalloidin/DAPI Staining)

Actin filaments in corneal keratocytes were investigated by Alexa Fluor™ 488-conjugated phalloidin, that attaches to the filamentous actin (F-actin) [91] after treatments with 50 $\mu g$/mL AME, $3x10^5$ Exo/mL and 50 $\mu g$/mL AME + $3x10^5$ Exo/mL.

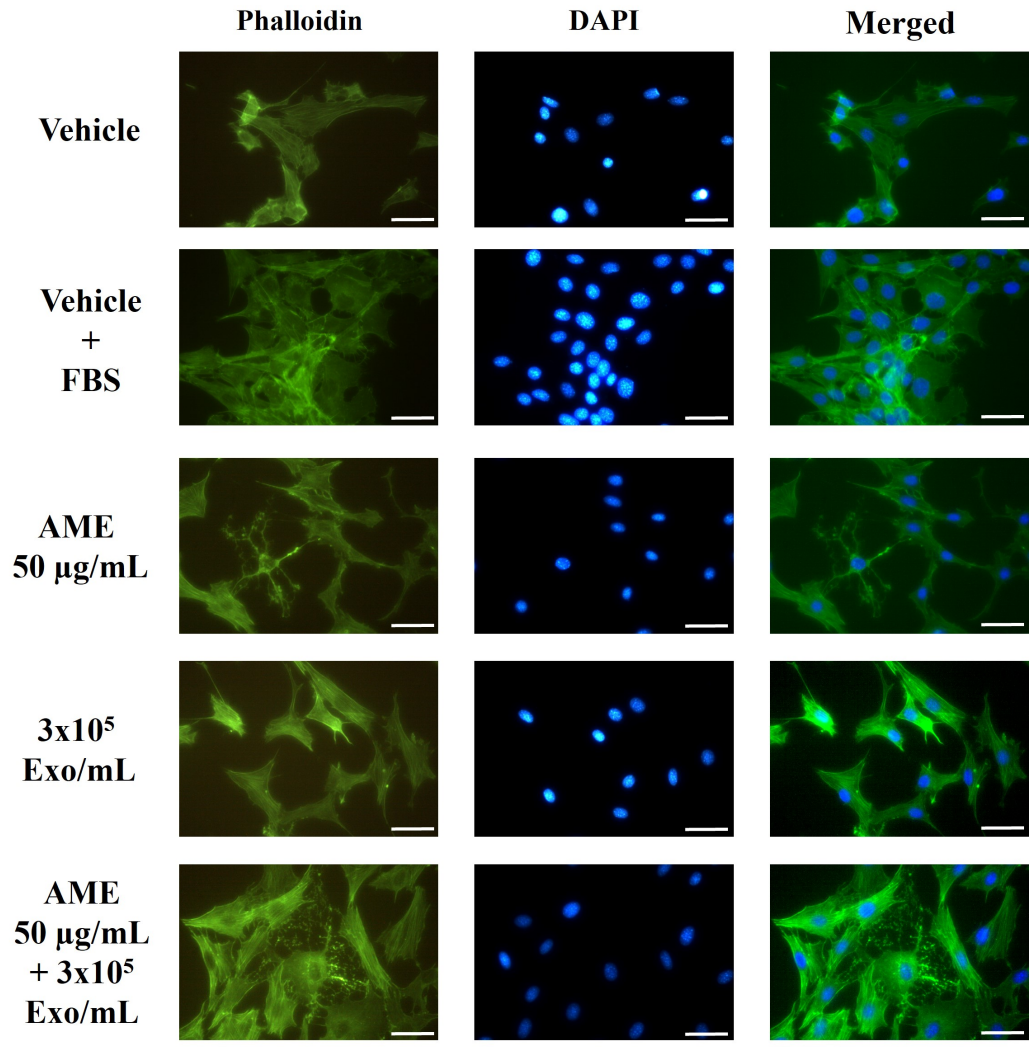


**Figure 4.5** Fluorescent staining of adherent human corneal keratocytes at day 2 on tissue culture plates treated with 50 $\mu g$/mL AME, 3x$10^5$ Exo/mL, 50 $\mu g$/mL AME and 3x$10^5$ Exo/mL, vehicle control (serum free culturing medium), and vehicle+ FBS (culturing medium contains 10% FBS), stained with conjugated phalloidin (Alexa Fluor™ 488 Phalloidin) and DAPI, Green colour indicates the actin cytoskeleton and blue colour indicates the nuclei. Scale bars: 50 $\mu m$.

Cellular morphologies were similar between experimental groups in general; however, larger cell bodies in serum supplemented media as well as with on keratocytes treated with AME and Exo together (Vehicle+FBS and 50 $\mu g$/mL AME + 3x$10^5$ Exo/mL). Dendritic-like protrusions have been observed on some cells in the presence of AME (50 $\mu g$/mL AME and 50 $\mu g$/mL AME + 3x$10^5$ Exo/mL)(Figure 4.5).

### 4.7.5 *In Vitro* Scratch Assay / Cell Migration Assay

Wound closure and cellular migration behaviour were evaluated via an *in vitro* scratch assay. Cells were imaged immediately after wound creation, and after 24 hours of treatments with serum free growth medium (vehicle), 50 $\mu g$/mL AME, 3x$10^5$ Exo/mL, 50 $\mu g$/mL AME + 3x$10^5$ Exo/mL in triplicates (n=3). Representative cell images and their binarized versions at 0 h and after 24 h were presented in Figure 4.6 A. Wound closure ratio was significantly higher in corneal keratocytes treated with mixture group (50 $\mu g$/mL AME + 3x$10^5$ Exo/mL) compared to cells treated with only 3x$10^5$ Exo/mL after 24 hours (*$p<0.05$) (Figure 4.6 B).

Visualization of the effects of different treatments on cell migration were depicted with staining of actin filaments of corneal keratocytes 48 hours after wound creation (Figure 4.7).

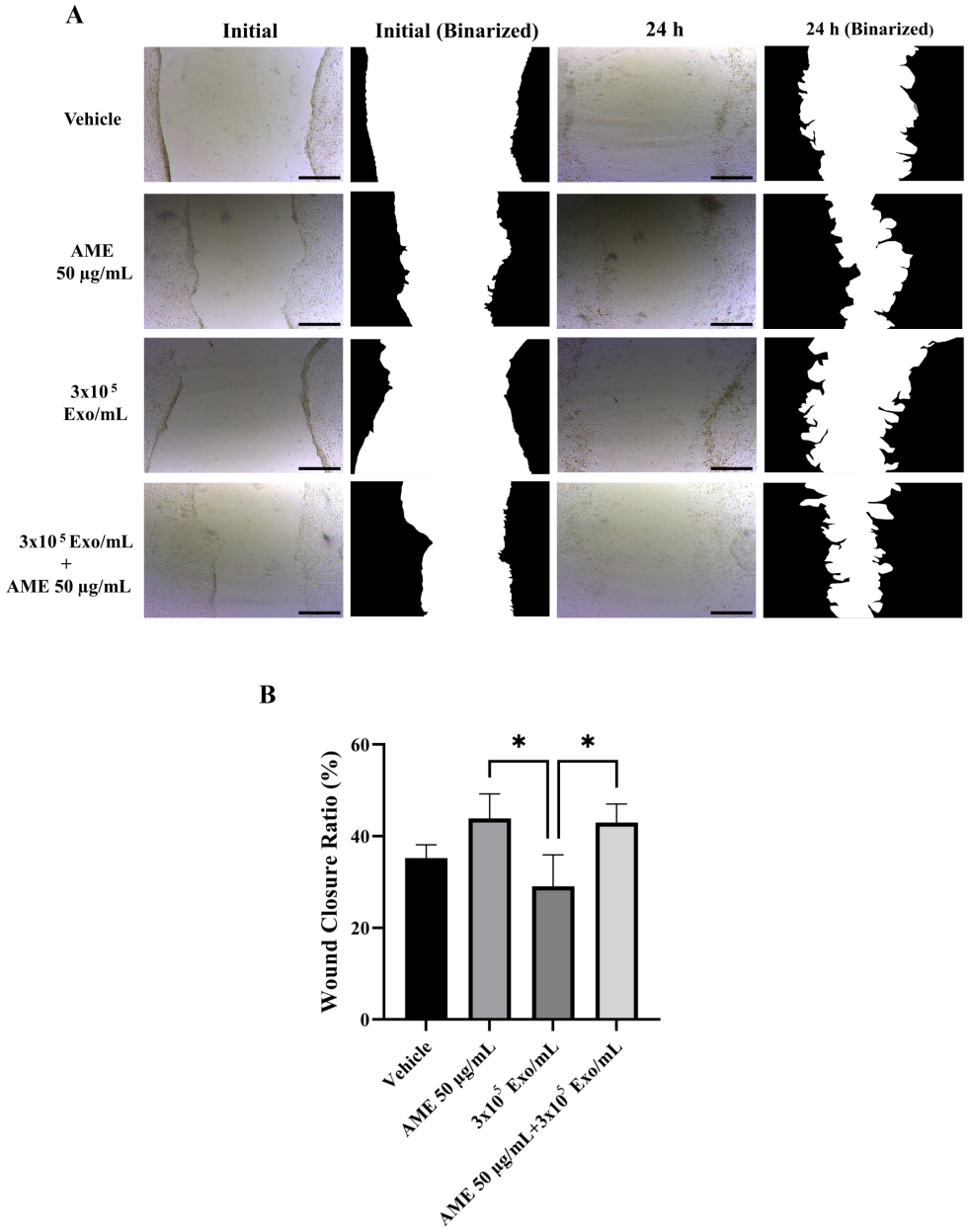


**Figure 4.6** Scratch assay on corneal keratocytes depicting wound closure ratios after treatments with 50 $\mu g$/mL AME, 3x10$^5$ Exo/mL and 50 $\mu g$/mL AME+ 3x10$^5$ Exo/mL. A) Representative cell images at initial wound creation and after 24 hours of treatment. (Scale bar: 500 $\mu m$) B) Wound Closure ratio (%). Scratch assay on corneal keratocytes indicates significantly higher wound closure in cells treated with 50 $\mu g$/mL AME + 3x10$^5$ Exo/mL compared to cells treated with only 3x10$^5$ after 24 hours (*p$<$0.05).

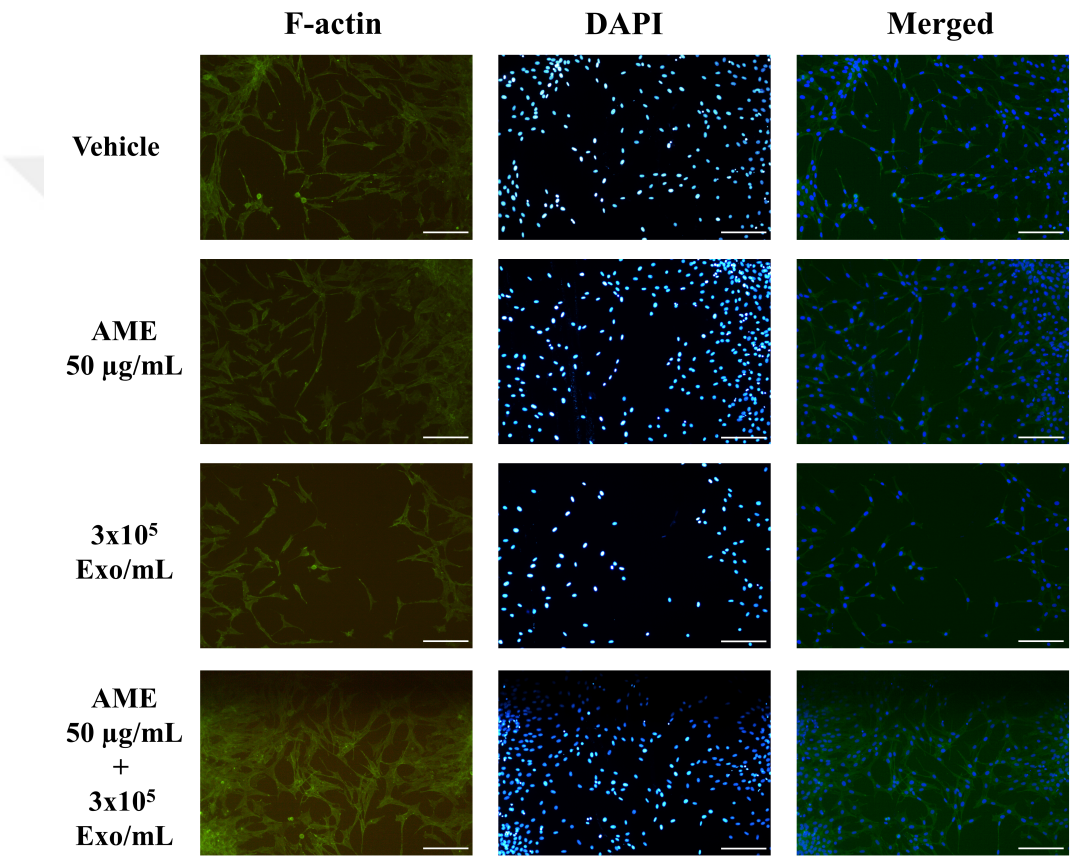


**Figure 4.7** Fluorescent staining of adherent human corneal keratocytes on tissue culture plates after scratch assay showing that cell migration after treatments with 50 $\mu g$/mL AME, 3x10$^5$ Exo/mL and their mixture. Images were taken 48 hours after the creation of the wound. Green colour indicates the actin cytoskeleton and blue colour indicates the nuclei (Scale bar: 200 $\mu m$).

## 4.8 Discussion

Exosomes from different sources (such as blood, saliva, breast milk, amniotic fluids) or cell types (fibroblasts, mesenchymal stem cells, tumor cells) may have different properties because of their cargo; such as, nucleic acids, signaling proteins, and metabolites [92]. This results in exosomes being highly heterogeneous in terms of their size, content, and functional effects for the recipient cells. Exosomes show a diameter ranging from 30 to 200 nanometers, encompassing a broad size spectrum [16]. Based on DLS analysis, the average size of Exos was 152.8 $\pm$ 7.701 nm. ESEM imaging also revealed that our exosomes (166.73 $\pm$ 40.35 nm) have a spherical and uniform morphology (Figure 4.2). In this thesis, ESEM and DLS techniques were utilised for the characterization of exosomes. Characterizing these samples using DLS may lead to overestimation or underestimation of particle sizes and this situation can be considered among the risks of using DLS for characterization. The presence of particles larger than the average size seen in ESEM may be due to the presence of impurities like protein aggregates, other nanoparticles, or other extracellular vesicles. In addition, the exosome suspension received from the company was thawed once to be divided into 50 $\mu L$ aliquots and kept at -80 °C until further use. All further uses and characterizations were performed immediately after the aliquots were thawed. This freezing-thawing process and the absence of any cryoprotectant during this process may have caused aggregation or fusion of exosomes and increased particle sizes [93, 94]. Transmission Electron Microscopy (TEM) and Nanoparticle Tracking Analysis (NTA) could also be utilised to obtain more comprehensive and accurate characterization of exosome samples. In addition, expression of some surface proteins like CD9 and CD63 is a crucial parameter used to identify and characterize exosomes and could be determined using Western Blot analysis [20]. However, since we obtained exosomes through commercial means, manufacturer claimed to perform related characterizations such as immunophenotypic analysis, so no further characterizations were performed after receiving exosomes.

*In vitro* analyses were performed after characterization studies of both Exo and AME. L929 fibroblast cells were employed to evaluate the safety and efficacy of various concentrations of AME. In a range of concentrations between 28 to 140 $\mu g$/mL, no

statistically significant different effect of AME was detected on the viability of L929 cells (ns: $p \geq 0.05$) (Figure 4.3). 50 $\mu g$/mL AME concentration was chosen within this concentration range for the further experiments. In a previous study, AME has been used in various concentrations (ranging from 0-160 $\mu g$/mL) and forms (as liquid drops, in situ gels, and tablets) for corneal repair [95]. However, our results show that concentrations above 280 $\mu g$/mL (280 $\mu g$/mL and 700 $\mu g$/mL) reduce cell viability, possibly due to cytotoxicity, demonstrating the necessity to determine the optimum concentration for the intended use. A similar result has been reported, and it was concluded that the possible reason for the negative effects of higher concentrations of AME on cell viability may be because of raised levels of inhibitory factors like transforming growth factor-beta (TGF-$\beta$) existing in AME [67]. In another study, it was also stated that AME has dose dependent effects on cellular behavior, therefore it is necessary to prevent the accumulation of growth factors [12].

Two different exosome concentrations were applied to corneal keratocytes. There were no significant statistical differences found between cell proliferation of corneal keratocytes treated with $3x10^5$ Exo/mL and $3x10^6$ Exo/mL concentrations both on day 2 and on day 3; therefore, $3x10^5$ Exo/mL concentration was selected for combination treatment with AME. Cell proliferation for both concentrations of exosomes were decreased on day 3 of culture (Figure 4.4 A). Since exosome treatment solutions were prepared by the dilution of serum-free growth medium, protein content needed by the cells in the medium may have been depleted after day 2 for optimal growth. The absence of serum, which provides essential nutrients, hormones and growth factors that support cell proliferation, may have caused a decrease in cell proliferation. In many publications, exosome concentration was given in $\mu g$/mL rather than as particle amount per mL [96]. Therefore, the exact particle amounts applied to the keratinocytes were not specified. In a study that compared the effects of WJ-MSC-Exos and AD-MSC-Exos on keratinocyte cell behaviour, 15% FBS contained growth medium was utilized for the experiment and 0 $\mu g$/mL, 0.1 $\mu g$/mL, 1 $\mu g$/mL, and 10 $\mu g$/mL exosome concentrations were applied on cells. Cell proliferation was evaluated at 48h and was higher in the cell groups that treated with WJ-MSC-Exos. Data for day 3 was not provided [81]. In also our results, exosome application increased proliferation on the

second day. Another reason for the decrease in cell proliferation after the 3rd day on only exosome applied group, may have been the induction of differentiation. Certain exosomes transmit signals that either promote cell cycle arrest or induce differentiation. As a result, the proliferation rate gradually decreases as cells exit the cell cycle and transition to a more differentiated state.

When both Exo (3x$10^5$ Exo/mL) and AME (50 $\mu g$/mL) solutions applied together as a mixture, cell proliferation on day 3 have increased significantly compared to both 50 $\mu g$/mL AME group and 3x$10^5$ Exo/mL group on day 3 (**** $p<0.0001$) (Figure 4.4 B). Combined use of AME and Exo solutions had a synergistically enhancing effect on corneal keratocyte proliferation. Exosomes initially promoted cell proliferation; however, their standalone utilization for long-term studies may not be sufficient, as indicated by the Alamar Blue assay results (Figure 4.4 B). When combined with AME, a more favorable outcome is observed compared to using AME alone.

Corneal keratocytes are quiescent cells with stellate/dendritic morphology in their native environment that can differentiate into corneal fibroblasts and myofibroblasts in a corneal damage event and can differentiate back to their original state afterwards [97]. Serum containing cell culturing media are reported to affect these cells to undergo into a fibroblastic differentiation route [46]. Staining of actin cytoskeleton of adherent corneal keratocytes in the presence and in the absence of Exo and AME were depicted in Figure 4.5. After culturing corneal keratocytes with serum containing medium, effect of 3x$10^5$ Exo/mL, 50 $\mu g$/mL AME, 3x$10^5$ Exo/mL + 50 $\mu g$/mL AME, and vehicle control (serum-free medium) was investigated in terms of their morphology. Actin cytoskeleton structures were generally identical to each other between experimental groups; however, it was observed that the keratocytes which were treated with serum supplemented media (Vehicle + FBS) have exhibited larger cell bodies compared to those which were treated with serum-free media. Similar morphological changes were also observed on keratocytes supplemented with both AME and Exo (50 $\mu g$/mL AME + 3x$10^5$ Exo/mL). Interestingly, presence of AME in culture medium on both isolated application of AME and combined application of AME + Exo (50 $\mu g$/mL AME + 3x$10^5$ Exo/mL) have resulted in an actin cytoskeletal morphology that resem-

bles dendritic protrusions in some areas of the culture. However, this observation might not be enough to represent entire population and have only been seen occasionally. Presence of AME may have caused changes in morphology in certain regions, similar morphological alterations have been observed in the literature in the presence of amniotic membrane proteins [98]. On the other hand, morphology and function of corneal keratocyte are also related with extracellular matrix (ECM) structure, topography, protein composition, and stiffness [99, 100]. Maruri *et al.* carried out a study which investigates the effects of ECM stiffness on corneal keratocytes' morphology in the presence or absence of TGF-$\beta$1. Results of this study indicates that soft gels (1 kPa) cause to be more dendritic cellular morphology in the presence of TGF-$\beta$1 while corneal keratocytes on stiff gels (10 kPa) or collagen coated glass coverslips have broad morphologies, generate many stress fibers, and show increased levels of $\alpha$-smooth muscle actin ($\alpha$-SMA) expression ($\alpha$-SMA is a crucial indicative for excessive scarring). In the same study, it was stated that without TGF-$\beta$1, stiff microenvironment alone is inadequate to stimulate activation of keratocyte into myofibroblast [100]. Conducting experiments on stiff polystyrene cell culture plates without any ECM protein coating, as in our study, may be insufficient to observe overall phenotypic changes in corneal keratocytes. Hence, the presence of AME and Exo alone may not be sufficient to make a definitive inference regarding cellular morphology.

To evaluate *in vitro* wound healing behavior, wound closure rates were quantified by pixel counts on binarized micrographs of wound areas. Corneal keratocytes showed higher wound closure rate after 3x$10^5$ Exo/mL+ 50 $\mu g$/mL AME application when compared to the only 3x$10^5$ Exo/mL treated group. Isolated 50 $\mu g$/mL AME application slightly increased wound closure rate but significant difference was not observed compared to the vehicle control (Figure 4.6). Individual uses of commercial AME [67] and MSC-derived exosomes [101] have previously been documented to enhance rate of wound repair in human corneal epithelial cells (HCEs). While we observed that both AME and AME+Exo individually improved cell proliferation compared to vehicle (**** $p<0.0001$), we did not observe a similar trend in wound healing behavior. Wound closure rate increased after AME and AME+Exo treatment compared to vehicle, but the change was not statistically significant. However, both AME and

AME+Exo individually enhance wound healing compared to only Exo treatment group (* $p<0.05$). Sole Exo treatment exhibited no significant enhancement in wound closure rate (%) in comparison with the vehicle group (ns: $p\geq0.05$). This finding suggests that the amount of Exo used in our study was sufficient to affect cell proliferation but did not induce an additional remodeling/migration response to recruit surrounding cells to the wound site compared to other treatments. In a similar study from the literature, $1x10^8$ Exosome/mL (corneal mesenchymal stromal cell derived exosomes) concentration was able to increase wound healing rate of corneal cells *in vitro* [20]. Here, we show that Exo amounts as low as $3x10^5$ Exo/mL can be utilized to boost cell proliferation concomitantly with AME to augment corneal wound healing *in vitro*.

A comparison of the tendency for scar tissue formation for each experimental group would be a very useful and meaningful experiment. It is known that TGF-$\beta$ encourages the accumulation of excess extracellular matrix (ECM) in the wound area, which can lead to scar formation. The expression of TGF-$\beta$1 and 2, an important pro-fibrotic cytokine, could be measured by quantitative PCR (qPCR). In addition, it would also be very useful to be able to perform various immunostainings to determine whether the applications of AME, Exo and their mixture cause keratocytes to differentiate into myofibroblasts, which are key cells in wound formation. For example, immunostaining could be performed for $\alpha$-Smooth Muscle Actin ($\alpha$-SMA), which is highly expressed by myofibroblasts [50].Immunostaining and Western Blot experiments required to identify some proteins generally expressed by keratocytes like Vimentin, Keratocan, Lumican [102, 103] could not be performed. The inability to perform some such experiments like immunostainings, Western Blot and qPCR can be listed as limitations of the thesis study.

# 5. CONCLUSION

In the first section of this thesis, HAM was characterized, and different forms of HAM were created. HAM can be utilised in different forms and strategies towards corneal regeneration, intact form of HAM, micron sized HAM particles, extract form and in combination with other polymeric materials. In this thesis, the extract form of HAM, AME, was mainly used alone and in combination with artificial eye drops. Combined use of AME and eye drop contained PVA (1.4%) and povidone (0.6%) significantly increased corneal keratocyte proliferation. Nevertheless, additional research is necessary to validate the advantages of using a combination of AME, and PVA-containing eye drops for promoting corneal keratocyte proliferation, and corneal wound healing. In addition, studies on the combination of eye drops containing HA and AME can be carried out as future studies.

In the second part of the thesis, AME concentration range and the amount of exosomes have been optimized for corneal keratocyte proliferation and their combined effects on corneal wound healing process. We observed that incorporating optimized concentrations of AME and number of exosomes together have significantly increased the rate of corneal keratocyte proliferation with no adverse effect on wound healing. Observations of actin cytoskeleton across combined and individual uses of AME and Exo have revealed that this synergistic approach can be utilized to investigate corneal keratocyte wound healing without major alteration to cellular morphology. Combination of AME and Exo on wound healing is not employed extensively in the literature. This synergistic effect can prove to be a promising tool for wound healing research on various other tissues. Nevertheless, more in-depth explorations on the changes of cellular behaviour in the presence of this synergistic effect would help to wound healing research.

# APPENDIX A. CALIBRATION CURVES

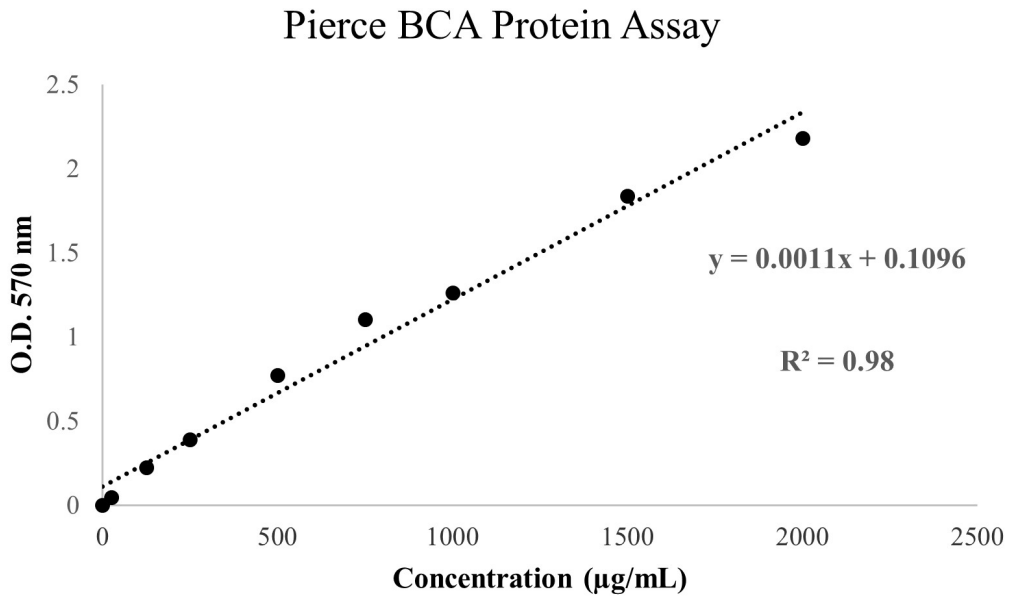


**Figure A.1** Calibration curve for Pierce™ BCA Protein Assay generated to determine AME concentration (Second batch of AME aliquots).

# REFERENCES


1. Arrizabalaga, J. H., and M. U. Nollert, "Human amniotic membrane: a versatile scaffold for tissue engineering," *ACS Biomaterials Science & Engineering*, Vol. 4, no. 7, pp. 2226–2236, 2018.

2. Elkhenany, H., A. El-Derby, M. Abd Elkodous, R. A. Salah, and *et al.*, "Applications of the amniotic membrane in tissue engineering and regeneration: the hundred-year challenge," *Stem Cell Research & Therapy*, Vol. 13, pp. 1–19, 2022.

3. Fénelon, M., S. Catros, C. Meyer, J.-C. Fricain, and *et al.*, "Applications of human amniotic membrane for tissue engineering," *Membranes*, Vol. 11, no. 6, p. 387, 2021.

4. Hariya, T., Y. Tanaka, S. Yokokura, and T. Nakazawa, "Transparent, resilient human amniotic membrane laminates for corneal transplantation," *Biomaterials*, Vol. 101, pp. 76–85, 2016.

5. Ji, S.-z., S.-c. Xiao, P.-f. Luo, G.-f. Huang, and *et al.*, "An epidermal stem cells niche microenvironment created by engineered human amniotic membrane," *Biomaterials*, Vol. 32, no. 31, pp. 7801–7811, 2011.

6. Murri, M. S., M. Moshirfar, O. C. Birdsong, Y. C. Ronquillo, and *et al.*, "Amniotic membrane extract and eye drops: a review of literature and clinical application," *Clinical Ophthalmology*, pp. 1105–1112, 2018.

7. Leal-Marin, S., T. Kern, N. Hofmann, O. Pogozhykh, and *et al.*, "Human amniotic membrane: A review on tissue engineering, application, and storage," *Journal of Biomedical Materials Research Part B: Applied Biomaterials*, Vol. 109, no. 8, pp. 1198–1215, 2021.

8. Yang, Y., Y. Zhang, Y. Yan, Q. Ji, and *et al.*, "A sponge-like double-layer wound dressing with chitosan and decellularized bovine amniotic membrane for promoting diabetic wound healing," *Polymers*, Vol. 12, no. 3, p. 535, 2020.

9. Uchino, Y., S. Shimmura, H. Miyashita, T. Taguchi, and *et al.*, "Amniotic membrane immobilized poly (vinyl alcohol) hybrid polymer as an artificial cornea scaffold that supports a stratified and differentiated corneal epithelium," *Journal of Biomedical Materials Research Part B: Applied Biomaterials*, Vol. 81, no. 1, pp. 201–206, 2007.

10. Zhang, Q., C. Qian, W. Xiao, and a. t. Zhu, Huajun, "Development of a visible light, cross-linked gelma hydrogel containing decellularized human amniotic particles as a soft tissue replacement for oral mucosa repair," *RSC Advances*, Vol. 9, no. 32, pp. 18344–18352, 2019.

11. He, H., W. Li, S.-Y. Chen, S. Zhang, and *et al.*, "Suppression of activation and induction of apoptosis in raw264. 7 cells by amniotic membrane extract," *Investigative Ophthalmology & Visual Science*, Vol. 49, no. 10, pp. 4468–4475, 2008.

12. Asl, N. S., F. Nejat, P. Mohammadi, A. Nekoukar, and *et al.*, "Amniotic membrane extract eye drop promotes limbal stem cell proliferation and corneal epithelium healing," *Cell Journal (Yakhteh)*, Vol. 20, no. 4, p. 459, 2019.

13. Murphy, S. V., A. Skardal, L. Song, K. Sutton, and *et al.*, "Solubilized amnion membrane hyaluronic acid hydrogel accelerates full-thickness wound healing," *Stem cells Translational Medicine*, Vol. 6, no. 11, pp. 2020–2032, 2017.

14. Fu-Shin, X. Y., J. Yin, K. Xu, and J. Huang, "Growth factors and corneal epithelial wound healing," *Brain Research Bulletin*, Vol. 81, no. 2-3, pp. 229–235, 2010.

15. Guo, Q., J. Hao, Q. Yang, L. Guan, and *et al.*, "A comparison of the effectiveness between amniotic membrane homogenate and transplanted amniotic membrane in healing corneal damage in a rabbit model," *Acta Ophthalmologica*, Vol. 89, no. 4, pp. e315–e319, 2011.

16. Gurung, S., D. Perocheau, L. Touramanidou, and J. Baruteau, "The exosome journey: from biogenesis to uptake and intracellular signalling," *Cell Communication and Signaling*, Vol. 19, no. 1, p. 47, 2021.

17. Kalluri, R., and V. S. LeBleu, "The biology, function, and biomedical applications of exosomes," *Science*, Vol. 367, no. 6478, p. 6977, 2020.

18. Zhang, Y., J. Bi, J. Huang, Y. Tang, and *et al.*, "Exosome: a review of its classification, isolation techniques, storage, diagnostic and targeted therapy applications," *International Journal of Nanomedicine*, pp. 6917–6934, 2020.

19. Safari, B., M. Aghazadeh, S. Davaran, and L. Roshangar, "Exosome-loaded hydrogels: a new cell-free therapeutic approach for skin regeneration," *European Journal of Pharmaceutics and Biopharmaceutics*, Vol. 171, pp. 50–59, 2022.

20. Samaeekia, R., B. Rabiee, I. Putra, X. Shen, and *et al.*, "Effect of human corneal mesenchymal stromal cell-derived exosomes on corneal epithelial wound healing," *Investigative Ophthalmology & Visual Science*, Vol. 59, no. 12, pp. 5194–5200, 2018.

21. Han, K.-Y., J. A. Tran, J.-H. Chang, D. T. Azar, and *et al.*, "Potential role of corneal epithelial cell-derived exosomes in corneal wound healing and neovascularization," *Scientific Reports*, Vol. 7, no. 1, p. 40548, 2017.

22. Wang, S., Y. Hou, X. Li, Z. Song, and *et al.*, "Comparison of exosomes derived from induced pluripotent stem cells and mesenchymal stem cells as therapeutic nanoparticles for treatment of corneal epithelial defects," *Aging (Albany NY)*, Vol. 12, no. 19, p. 19546, 2020.

23. Taghavi-Farahabadi, M., M. Mahmoudi, N. Rezaei, and S. M. Hashemi, "Whartonâs jelly mesenchymal stem cells exosomes and conditioned media increased neutrophil lifespan and phagocytosis capacity," *Immunological Investigations*, Vol. 50, no. 8, pp. 1042–1057, 2021.

24. Zhao, G., F. Liu, Z. Liu, K. Zuo, and *et al.*, "Msc-derived exosomes attenuate cell death through suppressing aif nucleus translocation and enhance cutaneous wound healing," *Stem Cell Research & Therapy*, Vol. 11, pp. 1–18, 2020.

25. Xiao, S., C. Xiao, Y. Miao, J. Wang, and *et al.*, "Human acellular amniotic membrane incorporating exosomes from adipose-derived mesenchymal stem cells promotes diabetic wound healing," *Stem Cell Research & Therapy*, Vol. 12, no. 1, p. 255, 2021.

26. Zhou, Z., J. Xun, C. Wu, C. Ji, and *et al.*, "Acceleration of burn wound healing by micronized amniotic membrane seeded with umbilical cord-derived mesenchymal stem cells," *Materials Today Bio*, Vol. 20, p. 100686, 2023.

27. Willoughby, C. E., D. Ponzin, S. Ferrari, and a. t. Lobo, Aires, "Anatomy and physiology of the human eye: effects of mucopolysaccharidoses disease on structure and function–a review," *Clinical & Experimental Ophthalmology*, Vol. 38, pp. 2–11, 2010.

28. Rüfer, F., A. Schröder, and C. Erb, "White-to-white corneal diameter: normal values in healthy humans obtained with the orbscan ii topography system," *Cornea*, Vol. 24, no. 3, pp. 259–261, 2005.

29. Sridhar, M. S., "Anatomy of cornea and ocular surface," *Indian journal of Ophthalmology*, Vol. 66, no. 2, pp. 190–194, 2018.

30. Meek, K. M., and C. Knupp, "Corneal structure and transparency," *Progress in Retinal and Eye Research*, Vol. 49, pp. 1–16, 2015.

31. Torricelli, A. A., V. Singh, M. R. Santhiago, and S. E. Wilson, "The corneal epithelial basement membrane: structure, function, and disease," *Investigative Ophthalmology & Visual Science*, Vol. 54, no. 9, pp. 6390–6400, 2013.

32. Wilson, S. E., A. A. Torricelli, and G. K. Marino, "Corneal epithelial basement membrane: Structure, function and regeneration," *Experimental Eye Research*, Vol. 194, p. 108002, 2020.

33. Rowsey, T. G., and D. Karamichos, "The role of lipids in corneal diseases and dystrophies: a systematic review," *Clinical and Translational Medicine*, Vol. 6, pp. 1–13, 2017.

34. Wilson, S. E., "Bowman's layer in the cornea–structure and function and regeneration," *Experimental Eye Research*, Vol. 195, p. 108033, 2020.

35. Espana, E. M., and D. E. Birk, "Composition, structure and function of the corneal stroma," *Experimental Eye Research*, Vol. 198, p. 108137, 2020.

36. de Oliveira, R. C., and S. E. Wilson, "Descemet's membrane development, structure, function and regeneration," *Experimental Eye Research*, Vol. 197, p. 108090, 2020.

37. Di Mundo, R., G. Recchia, M. Parekh, A. Ruzza, and *et al.*, "Sensing inhomogeneous mechanical properties of human corneal descemet's membrane with afm nano-indentation," *Journal of the Mechanical Behavior of Biomedical Materials*, Vol. 74, pp. 21–27, 2017.

38. Bourne, W., "Biology of the corneal endothelium in health and disease," *Eye*, Vol. 17, no. 8, pp. 912–918, 2003.

39. Sanchis-Gimeno, J., A. Lleo-Perez, L. Alonso, M. Rahhal, and F. Martinez Soriano, "Corneal endothelial cell density decreases with age in emmetropic eyes," *Histology and Histopathology*, 2005.

40. Hertsenberg, A. J., and J. L. Funderburgh, "Stem cells in the cornea," *Progress in Molecular Biology and Translational Science*, Vol. 134, pp. 25–41, 2015.

41. Jester, J. V., T. Moller-Pedersen, J. Huang, C. M. Sax, and *et al.*, "The cellular basis of corneal transparency: evidence for âcorneal crystallinsâ," *Journal of Cell Science*, Vol. 112, no. 5, pp. 613–622, 1999.

42. West-Mays, J. A., and D. J. Dwivedi, "The keratocyte: corneal stromal cell with variable repair phenotypes," *The international Journal of Biochemistry & Cell Biology*, Vol. 38, no. 10, pp. 1625–1631, 2006.

43. Fukuda, K., "Corneal fibroblasts: Function and markers," *Experimental Eye Research*, Vol. 200, p. 108229, 2020.

44. Fini, M. E., and B. M. Stramer, "How the cornea heals: cornea-specific repair mechanisms affecting surgical outcomes," *Cornea*, Vol. 24, no. 8, pp. S2–S11, 2005.

45. Yam, G. H.-F., M. Fuest, N. Z. B. M. Yusoff, T.-W. Goh, and *et al.*, "Safety and feasibility of intrastromal injection of cultivated human corneal stromal keratocytes as cell-based therapy for corneal opacities," *Investigative Ophthalmology & Visual Science*, Vol. 59, no. 8, pp. 3340–3354, 2018.

46. Fini, M. E., "Keratocyte and fibroblast phenotypes in the repairing cornea," *Progress in Retinal and Eye Research*, Vol. 18, no. 4, pp. 529–551, 1999.

47. Espana, E. M., H. He, T. Kawakita, M. A. Di Pascuale, and *et al.*, "Human keratocytes cultured on amniotic membrane stroma preserve morphology and express keratocan," *Investigative Ophthalmology & Visual Science*, Vol. 44, no. 12, pp. 5136–5141, 2003.

48. Li, W., H. He, Y.-T. Chen, Y. Hayashida, and *et al.*, "Reversal of myofibroblasts by amniotic membrane stromal extract," *Journal of Cellular Physiology*, Vol. 215, no. 3, pp. 657–664, 2008.

49. Che, X., H. Wu, C. Jia, H. Sun, and *et al.*, "A novel tissue-engineered corneal stromal equivalent based on amniotic membrane and keratocytes," *Investigative Ophthalmology & Visual Science*, Vol. 60, no. 2, pp. 517–527, 2019.

50. Ljubimov, A. V., and M. Saghizadeh, "Progress in corneal wound healing," *Progress in Retinal and Eye Research*, Vol. 49, pp. 17–45, 2015.

51. Kamil, S., and R. R. Mohan, "Corneal stromal wound healing: Major regulators and therapeutic targets," *The Ocular Surface*, Vol. 19, pp. 290–306, 2021.

52. Eraslan, M., and E. Toker, "Mechanisms of corneal wound healing and its modulation following refractive surgery," *Marmara Med. J*, Vol. 22, no. 2, pp. 169–187, 2009.

53. Hossain, L., M. Arifuzzaman, F. Diba, A. Siddika, and *et al.*, "Human amniotic membrane preparation, preservation and clinical application using various techniques for the treatment of ophthalmic dysfunctions," *Preprints*, 2018.

54. Malhotra, C., and A. K. Jain, "Human amniotic membrane transplantation: different modalities of its use in ophthalmology," *World Journal of Transplantation*, Vol. 4, no. 2, p. 111, 2014.

55. Koizumi, N., T. Inatomi, C. Sotozono, N. J. Fullwood, and *et al.*, "Growth factor mrna and protein in preserved human amniotic membrane," *Current Eye Research*, Vol. 20, no. 3, pp. 173–177, 2000.

56. Gholipourmalekabadi, M., B. Farhadihosseinabadi, M. Faraji, and M. R. Nourani, "How preparation and preservation procedures affect the properties of amniotic membrane? how safe are the procedures?," *Burns*, Vol. 46, no. 6, pp. 1254–1271, 2020.

57. Spoerl, E., G. Wollensak, F. Reber, and L. Pillunat, "Cross-linking of human amniotic membrane by glutaraldehyde," *Ophthalmic Research*, Vol. 36, no. 2, pp. 71–77, 2004.

58. Sekar, S., K. Sasirekha, S. Krishnakumar, and T. Sastry, "A novel cross-linked human amniotic membrane for corneal implantations," *Proceedings of the Institution of Mechanical Engineers, Part H: Journal of Engineering in Medicine*, Vol. 227, no. 3, pp. 221–228, 2013.

59. Jirsova, K., and G. L. Jones, "Amniotic membrane in ophthalmology: properties, preparation, storage and indications for graftingâa review," *Cell and Tissue Banking*, Vol. 18, pp. 193–204, 2017.

60. Sanluis-Verdes, A., N. Sanluis-Verdes, M. J. Manso-Revilla, A. M. Castro-Castro, and *et al.*, "Tissue engineering for neurodegenerative diseases using human amniotic membrane and umbilical cord," *Cell and Tissue Banking*, Vol. 18, pp. 1–15, 2017.

61. Wilshaw, S.-P., J. N. Kearney, J. Fisher, and E. Ingham, "Production of an acellular amniotic membrane matrix for use in tissue engineering," *Tissue Engineering*, Vol. 12, no. 8, pp. 2117–2129, 2006.

62. Saghizadeh, M., M. A. Winkler, A. A. Kramerov, D. M. Hemmati, and *et al.*, "A simple alkaline method for decellularizing human amniotic membrane for cell culture," *PloS One*, Vol. 8, no. 11, p. e79632, 2013.

63. Porzionato, A., E. Stocco, S. Barbon, F. Grandi, and *et al.*, "Tissue-engineered grafts from human decellularized extracellular matrices: a systematic review and future perspectives," *International Journal of Molecular Sciences*, Vol. 19, no. 12, p. 4117, 2018.

64. Dadkhah Tehrani, F., A. Firouzeh, I. Shabani, and A. Shabani, "A review on modifications of amniotic membrane for biomedical applications," *Frontiers in Bioengineering and Biotechnology*, Vol. 8, p. 606982, 2021.

65. Yang, E. K., J. K. Park, J. I. Ahn, H. G. Lee, and *et al.*, "Tissue-engineered skin substitutes using collagen scaffold with amniotic membrane component," *Key Engineering Materials*, Vol. 277, pp. 12–18, 2004.

66. Hortensius, R. A., J. H. Ebens, and B. A. Harley, "Immunomodulatory effects of amniotic membrane matrix incorporated into collagen scaffolds," *Journal of Biomedical Materials Research Part A*, Vol. 104, no. 6, pp. 1332–1342, 2016.

67. Dudok, D. V., I. Nagdee, K. Cheung, H. Liu, and *et al.*, "Effects of amniotic membrane extract on primary human corneal epithelial and limbal cells," *Clinical & Experimental Ophthalmology*, Vol. 43, no. 5, pp. 443–448, 2015.

68. Shabani, A., F. Atyabi, M. R. Khoshayand, Mahbod, and *et al.*, "Design of experiment, preparation, and in vitro biological assessment of human amniotic membrane extract loaded nanoparticles," *Current Pharmaceutical Biotechnology*, Vol. 21, no. 3, pp. 256–267, 2020.

69. Mohamed, H. B., B. N. Abd El-Hamid, D. Fathalla, and E. A. Fouad, "Current trends in pharmaceutical treatment of dry eye disease: A review," *European Journal of Pharmaceutical Sciences*, Vol. 175, p. 106206, 2022.

70. Kathuria, A., K. Shamloo, V. Jhanji, and A. Sharma, "Categorization of marketed artificial tear formulations based on their ingredients: a rational approach for their use," *Journal of Clinical Medicine*, Vol. 10, no. 6, p. 1289, 2021.

71. Zhang, Y., X.-Y. Lu, R.-J. Hu, F.-L. Fan, and *et al.*, "Evaluation of artificial tears on cornea epithelium healing," *International Journal of Ophthalmology*, Vol. 11, no. 7, p. 1096, 2018.

72. Joorabloo, A., and T. Liu, "Engineering exosome-based biomimetic nanovehicles for wound healing," *Journal of Controlled Release*, Vol. 356, pp. 463–480, 2023.

73. Hofmann, L., S. Ludwig, J. M. Vahl, C. Brunner, and *et al.*, "The emerging role of exosomes in diagnosis, prognosis, and therapy in head and neck cancer," *International Journal of Molecular Sciences*, Vol. 21, no. 11, p. 4072, 2020.

74. Shen, T., Q.-Q. Zheng, J. Shen, Q.-S. Li, and *et al.*, "Effects of adipose-derived mesenchymal stem cell exosomes on corneal stromal fibroblast viability and extracellular matrix synthesis," *Chinese Medical Journal*, Vol. 131, no. 06, pp. 704–712, 2018.

75. Kim, S., Y. Kim, Y.-S. Hyun, H. Choi, and *et al.*, "Exosomes from human cord blood plasma accelerate cutaneous wound healing by promoting fibroblast function, angiogenesis, and m2 macrophage differentiation," *Biomaterials Science*, Vol. 9, no. 8, pp. 3028–3039, 2021.

76. Sterzenbach, U., U. Putz, L.-H. Low, J. Silke, and *et al.*, "Engineered exosomes as vehicles for biologically active proteins," *Molecular Therapy*, Vol. 25, no. 6, pp. 1269–1278, 2017.

77. Wei, X., X. Li, Y. Zhang, J. Wang, and *et al.*, "Advances in the therapeutic applications of plant-derived exosomes in the treatment of inflammatory diseases," *Biomedicines*, Vol. 11, no. 6, p. 1554, 2023.

78. Sarasati, A., M. H. Syahruddin, A. Nuryanti, I. D. Ana, and *et al.*, "Plant-derived exosome-like nanoparticles for biomedical applications and regenerative therapy," *Biomedicines*, Vol. 11, no. 4, p. 1053, 2023.

79. Nemati, M., B. Singh, R. A. Mir, M. Nemati, and *et al.*, "Plant-derived extracellular vesicles: a novel nanomedicine approach with advantages and challenges," *Cell Communication and Signaling*, Vol. 20, no. 1, p. 69, 2022.

80. Théry, C., L. Zitvogel, and S. Amigorena, "Exosomes: composition, biogenesis and function," *Nature Reviews Immunology*, Vol. 2, no. 8, pp. 569–579, 2002.

81. Yu, H.-R., H.-C. Huang, I.-L. Chen, and S.-C. Li, "Exosomes secreted by whartonâs jelly-derived mesenchymal stem cells promote the ability of cell proliferation and migration for keratinocyte," *International Journal of Molecular Sciences*, Vol. 25, no. 9, p. 4758, 2024.

82. Bakhtyar, N., M. G. Jeschke, E. Herer, M. Sheikholeslam, and S. Amini-Nik, "Exosomes from acellular whartonâs jelly of the human umbilical cord promotes skin wound healing," *Stem Cell Research & Therapy*, Vol. 9, pp. 1–14, 2018.

83. Al Shehadat, S., M. O. Gorduysus, S. S. A. Hamid, N. A. Abdullah, and *et al.*, "Optimization of scanning electron microscope technique for amniotic membrane investigation: A preliminary study," *European Journal of Dentistry*, Vol. 12, no. 04, pp. 574–578, 2018.

84. Yamamoto, M., Y. Takahashi, and Y. Tabata, "Controlled release by biodegradable hydrogels enhances the ectopic bone formation of bone morphogenetic protein," *Biomaterials*, Vol. 24, no. 24, pp. 4375–4383, 2003.

85. Kim, J. C., and S. C. Tseng, "Transplantation of preserved human amniotic membrane for surface reconstruction in severely damaged rabbit corneas," *Cornea*, Vol. 14, no. 5, pp. 473–484, 1995.

86. Samarkanova, D., S. Cox, D. Hernandez, L. Rodriguez, and *et al.*, "Cord blood and amniotic membrane extract eye drop preparations display immune-suppressive and regenerative properties," *Scientific Reports*, Vol. 11, no. 1, p. 13754, 2021.

87. Fallacara, A., S. Vertuani, G. Panozzo, A. Pecorelli, and *et al.*, "Novel artificial tears containing cross-linked hyaluronic acid: an in vitro re-epithelialization study," *Molecules*, Vol. 22, no. 12, p. 2104, 2017.

88. Tang, X., H. Wu, J. Xie, N. Wang, Q. Chen, and *et al.*, "The combination of dextran sulphate and polyvinyl alcohol prevents excess aggregation and promotes proliferation of pluripotent stem cells in suspension culture," *Cell Proliferation*, Vol. 54, no. 9, p. e13112, 2021.

89. Wu, Z., B. Kong, R. Liu, W. Sun, and *et al.*, "Engineering of corneal tissue through an aligned pva/collagen composite nanofibrous electrospun scaffold," *Nanomaterials*, Vol. 8, no. 2, p. 124, 2018.

90. Liang, C.-C., A. Y. Park, and J.-L. Guan, "In vitro scratch assay: a convenient and inexpensive method for analysis of cell migration in vitro," *Nature Protocols*, Vol. 2, no. 2, pp. 329–333, 2007.

91. Chen, J., L. J. Backman, W. Zhang, C. Ling, and *et al.*, "Regulation of keratocyte phenotype and cell behavior by substrate stiffness," *ACS Biomaterials Science & Engineering*, Vol. 6, no. 9, pp. 5162–5171, 2020.

92. Kimiz-Gebologlu, I., and S. S. Oncel, "Exosomes: Large-scale production, isolation, drug loading efficiency, and biodistribution and uptake," *Journal of Controlled Release*, Vol. 347, pp. 533–543, 2022.

93. Gelibter, S., G. Marostica, A. Mandelli, S. Siciliani, and *et al.*, "The impact of storage on extracellular vesicles: A systematic study," *Journal of Extracellular Vesicles*, Vol. 11, no. 2, p. e12162, 2022.

94. Sivanantham, A., and Y. Jin, "Impact of storage conditions on ev integrity/surface markers and cargos," *Life*, Vol. 12, no. 5, p. 697, 2022.

95. Luo, Y., M. Shen, P. Feng, H. Qiu, and *et al.*, "Various administration forms of decellularized amniotic membrane extract towards improving corneal repair," *Journal of Materials Chemistry B*, Vol. 9, no. 45, pp. 9347–9357, 2021.

96. Abas, B. I., G. M. Demirbolat, and O. Cevik, "Wharton jelly-derived mesenchymal stem cell exosomes induce apoptosis and suppress emt signaling in cervical cancer cells as an effective drug carrier system of paclitaxel," *PloS One*, Vol. 17, no. 9, p. e0274607, 2022.

97. Surovtseva, M. A., I. I. Kim, N. A. Bondarenko, A. P. Lykov, and *et al.*, "Derivation of human corneal keratocytes from relex smile lenticules for cell therapy and tissue engineering," *International Journal of Molecular Sciences*, Vol. 24, no. 10, p. 8828, 2023.

98. Zhu, Y.-T., F. Li, Y. Zhang, S.-Y. Chen, and *et al.*, "Hc-ha/ptx3 purified from human amniotic membrane reverts human corneal fibroblasts and myofibroblasts to keratocytes by activating bmp signaling," *Investigative Ophthalmology & Visual Science*, Vol. 61, no. 5, pp. 62–62, 2020.

99. Petroll, W. M., V. D. Varner, and D. W. Schmidtke, "Keratocyte mechanobiology," *Experimental Eye Research*, Vol. 200, p. 108228, 2020.

100. Maruri, D. P., M. Miron-Mendoza, P. B. Kivanany, J. M. Hack, Schmidtke, and *et al.*, "Ecm stiffness controls the activation and contractility of corneal keratocytes in response to tgf-$\beta$1," *Biophysical Journal*, Vol. 119, no. 9, pp. 1865–1877, 2020.

101. Tao, H., X. Chen, H. Cao, L. Zheng, and *et al.*, "Mesenchymal stem cell-derived extracellular vesicles for corneal wound repair," *Stem Cells International*, Vol. 2019, no. 1, p. 5738510, 2019.

102. Shen, T., Q. Zheng, H. Luo, X. Li, and *et al.*, "Exosomal mir-19a from adipose-derived stem cells suppresses differentiation of corneal keratocytes into myofibroblasts," *Aging (Albany NY)*, Vol. 12, no. 5, p. 4093, 2020.

103. Jester, J. V., D. Brown, A. Pappa, and V. Vasiliou, "Myofibroblast differentiation modulates keratocyte crystallin protein expression, concentration, and cellular light scattering," *Investigative Ophthalmology & Visual Science*, Vol. 53, no. 2, pp. 770–778, 2012.